Molecular Immunology 116 (2019) 140–150

Contents lists available at ScienceDirect

Molecular Immunology

journal homepage: www.elsevier.com/locate/molimm

Boiling down the cysteine-stabilized LTP fold - loss of structural and immunological integrity of allergenic Art v 3 and Pru p 3 as a consequence of irreversible lanthionine formation

Sabrina Wildner[a,b], Iris Griessner[a], Teresa Stemeseder[a], Christof Regl[a,b], Wai Tuck Soh[a], Lorenz G. Stock[a,b], Timo Völker[a,b], Claudia Alessandri[c], Adriano Mari[c], Christian G. Huber[a,b], Hanno Stutz[a,b], Hans Brandstetter[a,b], Gabriele Gadermaier[a,b,*]

[a] Department of Biosciences, University of Salzburg, Salzburg, Austria
[b] Christian Doppler Laboratory for Innovative Tools for the Characterization of Biosimilars, University of Salzburg, Salzburg, Austria
[c] Associated Centers for Molecular Allergology, Rome, Italy

ARTICLE INFO

Keywords:
Lipid transfer protein
Art v 3 crystal structure
Lanthionine
Thermal stability
Pru p 3
Buffer environment

ABSTRACT

Background: Non-specific lipid transfer proteins (LTPs) are important allergens in fruits, pollen, vegetables, nuts and latex. Due to their compact structure, LTPs are highly resistant to heat treatment. Here, Art v 3 from mugwort pollen and Pru p 3 from peach were used as model allergens to in-depth investigate structural and immunological properties upon thermal treatment at different buffer conditions.

Methods: Recombinant Art v 3 and Pru p 3 were purified from *E. coli* and incubated at 95 °C up to 120 min using sodium phosphate buffer pH 3.4 or 7.3. Physicochemical properties of allergens were analyzed in circular dichroism spectroscopy, Fourier transform infrared spectroscopy, dynamic light scattering, size exclusion chromatography, and mass spectrometry. The crystal structure of Art v 3.0201 was determined to 1.9 Å resolution. IgG and IgE binding was investigated in ELISA using murine and LTP allergic patients' sera.

Results: Highly pure and homogenous recombinant allergens were obtained from bacterial production. The crystal structure of Art v 3.0201 revealed an antiparallel four helix bundle with a C-terminal extension mediating an asymmetric, transient dimer interface and differently sized cavities. Both allergens showed high thermal stability at acidic conditions. In contrast, extensive heat treatment in neutral buffer induced irreversible structural changes due to lanthionine-based cysteine rearrangement. This fostered loss of the typical α-helical structure, increased molecular size and abrogation of IgG and IgE binding epitopes. Pru p 3 lost its structural integrity at shorter heat stress duration than Art v 3, which did however only partially affect the molecule's IgE binding epitopes.

Conclusion: During thermal treatment, susceptibility to structural changes of the LTP-fold is highly dependent on the surrounding environment but also on intrinsic features of individual LTPs. This is a crucial fact to consider when processing LTP-containing food or food products as this will directly influence their allergenic potential.

1. Introduction

Non-specific lipid transfer proteins (LTPs) type 1 are widely distributed in the plant kingdom presenting important allergens in fruits and vegetables, but also in pollen and latex. To date, more than 50 allergens of the LTP family are officially acknowledged by the WHO/IUIS Allergen Nomenclature Sub-Committee and the vast majority of them are food allergens. As LTPs are suggested to primary sensitize patients via the gastrointestinal route they are categorized as true food allergens (Egger et al., 2010; van Ree, 2002). They are small, basic proteins containing a characteristic α-helical structure stabilized via four disulfide bonds. The four α-helices form a hydrophobic cavity which can interact with different types of lipids and a function in transferring lipids between membranes was determined in vitro. Nevertheless, this biological function of LTPs is still debated as so far in vivo evidence is lacking and LTPs are primarily located extracellularly (Salcedo et al., 2007; Yeats and Rose, 2008). They belong to the pathogenesis-related (PR)-14 family, and a role in the defense against

* Corresponding author at: Department of Biosciences, Christian Doppler Laboratory for Biosimilar Characterization, University of Salzburg, Hellbrunner Straße 34, A-5020 Salzburg, Austria.
E-mail address: Gabriele.Gadermaier@sbg.ac.at (G. Gadermaier).

https://doi.org/10.1016/j.molimm.2019.10.012
Received 9 September 2019; Received in revised form 11 October 2019; Accepted 15 October 2019
0161-5890/ © 2019 Elsevier Ltd. All rights reserved.

bacterial, fungal or viral plant pathogens was proposed which depends on the presence of lipids and can activate the plant immune system via a receptor-dependent mechanism (Finkina et al., 2016; Scheurer and Schulke, 2018).

Two prototypic members of the LTP family are Art v 3 from mugwort (*Artemisia vulgaris)* and Pru p 3 from peach (*Prunus persica*). Art v 3 represents a relevant mugwort allergen with a sensitization prevalence up to 89% among *Artemisia vulgaris* pollen sensitized patients. Pru p 3 plays the most important role in LTP-mediated food allergies especially in the Mediterranean areas (Barber et al., 2008; Asero et al., 2018). Analysis of cross-reactivity between pollen and food allergens showed that Art v 3 at least partially cross-reacts with homologous proteins from chestnut, celery stalks, peach and hazelnut (Egger et al., 2010; Gadermaier et al., 2011a; Salcedo et al., 2004; Palacin et al., 2012). However, IgE cross-reactivity between the LTPs highly depends on the patient cohort and even individual patients. Several studies demonstrated that Pru p 3 acts as primary sensitizer and thus seems to be the key driver in sensitization to other LTPs (Zuidmeer and van Ree, 2007; Scala et al., 2015; Pastorello et al., 2002; Bernardi et al., 2011). On the other hand, studies from China and southern Europe revealed that allergy to peach could originate from primary sensitization to Art v 3 in some patients (Palacin et al., 2012; Gao et al., 2013; Lombardero et al., 2004). Therefore, it cannot be entirely ruled out that primary sensitization to pollen LTP can lead to food allergy within the LTP syndrome. Though plant non-specific LTP type 1 constitute relevant allergens, the structure of only a limited number of molecules from this family is available. Solved structures of allergenic representatives originate from peach, lentils, pea, and hazelnut, while also other non-allergenic plant food LTPs from *e. g.* potato, dill, barley, and rice were determined (Pasquato et al., 2006; Shenkarev et al., 2017; Bogdanov et al., 2016; Melnikova et al., 2016; Bakan et al., 2009; Offermann et al., 2015; Cheng et al., 2004; Jain and Salunke, 2017). So far, research has focused on plant food representatives and no structure of a pollen member has been resolved.

Members of the LTP family have a high resistance to thermal processing and proteolytic digestion due to their compact cysteine-stabilized fold (Asero et al., 2001). This particular high stability is considered crucial for the allergens to survive the harsh environment in the gastrointestinal tract and to reach the immune system in an immunogenic state. Some studies have recently demonstrated that LTPs can refold after heating in acidic environment. Therefore, LTPs are able to retain their allergenic capacity in thermally treated products like juice, jam and nectars, which was previously demonstrated for Pru p 3 (Duffort et al., 2002; Brenna et al., 2000; Sancho et al., 2005). Although LTPs are extremely heat stable, the secondary structure may be altered after heating at neutral pH conditions. In circular dichroism spectroscopy, irreversible changes in secondary structures depending on the buffer environment and concentration have been monitored for some LTPs (Gaier et al., 2008; Gadermaier et al., 2009, 2011b; Vejvar et al., 2013). However, none of the lipid transfer proteins have been investigated in detail regarding their structural characteristics and antibody binding profiles upon thermal processing at different environment conditions.

Within this work, we solved the first 3-dimensional structure of a pollen LTP, i.e. Art v 3. Structural alterations and dynamics of recombinant Art v 3 and Pru p 3 upon thermal treatment were monitored by circular dichroism spectroscopy, dynamic light scattering, Fourier transform infrared spectroscopy and mass spectrometry. In hand with IgE and IgG antibody reactivity profiles we were able to demonstrate intrinsic structural features established upon thermal processing of pollen and food LTPs.

2. Methods

2.1. Production of recombinant Art v 3 and Pru p 3

For production of non-tagged recombinant proteins, Art v 3.0201 in pHis Parallel2 and Pru p 3.0102 in pET26b were transformed into *E. coli* Rosetta gamiB and *E. coli* Rosetta gami2 pLysS (Novagen, Gibbstown, NJ, USA), respectively. Expression was induced with 0.4 mM isopropyl-β-D-thiogalactopyranoside at $OD_{600} = 0.6$ and cells were grown at 16 °C overnight. Proteins were extracted in 5 mM ammonium carbonate pH 7.4, 5 mM sodium chloride buffer and bacterial contaminants were precipitated by adding 10% acetic acid for adjustment to pH 3.9. Proteins were purified by cation exchange chromatography using a 1 ml SPFF column (GE Healthcare, Chalfont St. Giles, UK). After washing with 20 mM sodium acetate pH 3.9, fractions were collected during a 30 ml linear gradient elution to 20 mM sodium acetate pH 3.9, 1 M NaCl. Fractions containing purified Art v 3.0201 (Art v 3) or Pru p 3.0101 (Pru p 3) were pooled, lyophilized and stored at -20 °C until further use.

2.2. Gel electrophoresis

Proteins were analyzed by denaturing polyacrylamide gel electrophoresis (SDS-PAGE) using 15% mini-gels under reducing conditions and Coomassie Brilliant Blue G-250 (Bio-Rad, Hercules, CA, USA) was used for staining.

2.3. Intact mass spectrometry and amino acid analysis

Intact mass was determined on a Thermo Scientific™ Q Exactive™ Hybrid-Quadrupol-Orbitrap mass spectrometer. Detailed settings of mass spectrometry-based analysis are provided online. Amino acid analysis was performed in duplicates following the Pico-Tag™ method (Waters, Milford, MA, USA). Phenylthiocarbamyl amino acid derivatives were analyzed by reversed phase high-performance liquid chromatography (UltiMate 3000, Thermo Fischer, Waltham, MA, USA), using a 3.0 x 150 mm XSELECT™ HSS T3 3.5 µm column (Waters, Dublin, Ireland). Peaks of hydrolyzed amino acids were quantified at 254 nm by peak area comparison to amino acid standard H (Pierce, Rockford, IL, USA).

2.4. Crystallization and crystal structure determination

Purified Art v 3 was concentrated to 14 mg/ml in 10 mM Tris-HCl pH 7.5 and crystallized by the sitting-drop vapor diffusion method at 293 K. Crystals with dimensions of $0.1 \times 0.1 \times 0.2\ mm^3$ were obtained in a condition consisting of 0.1 M HEPES pH 7.0, 3.2 M ammonium sulfate within 2 weeks. Diffraction data were collected at the ESRF beamline ID29 to 1.9 Å resolution, Online Table 1. The data were integrated with the program MOSFLM and scaled and merged with SCALA software (Winn et al., 2011). The phase problem was solved by molecular replacement using PHASER using Pru p 3 structure (PDB:2ALG). Structure models were built using COOT and refined using REFMAC and PHENIX (Afonine et al., 2012; Emsley et al., 2010). Coordinates and data sets are deposited with the protein data bank (entry 6FRR). Cα-RMSD analysis was done using the ce-align algorithm in PyMOL (version 1.7.2). Ligand binding pockets of both Art v 3 molecules in the asymmetric unit were calculated individually using the POCASA version 1.1 web server (parameters: probe radius, 1 Å; SPF, 14; PDF, 18; grid size 1 Å) at http://altair.sci.hokudai.ac.jp/g6/service/pocasa/ (Yu et al., 2010).

2.5. Thermal treatment of Art v 3 and Pru p 3

Lyophilized aliquots of Art v 3 and Pru p 3 were dissolved at a protein concentration of 0.3 mg/ml in 10 mM sodium phosphate buffer

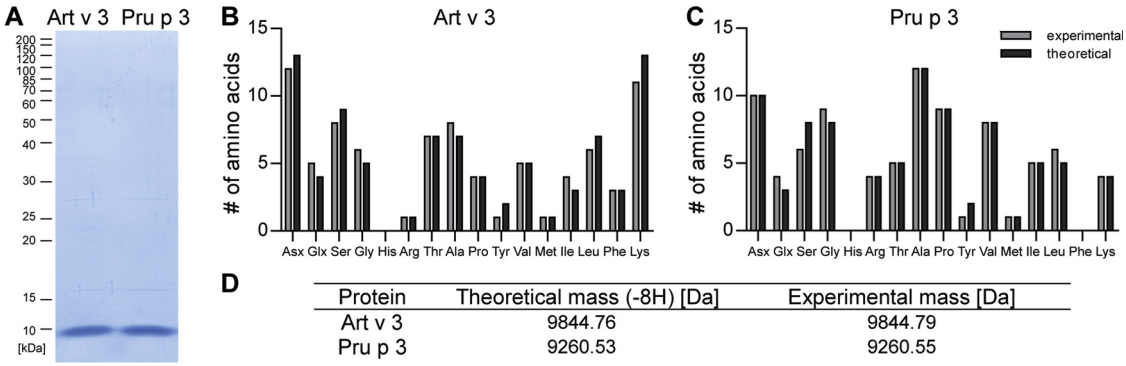

D

Protein	Theoretical mass (-8H) [Da]	Experimental mass [Da]
Art v 3	9844.76	9844.79
Pru p 3	9260.53	9260.55

Fig. 1. Characterization of recombinant LTPs. (A) Gel electrophoresis of Coomassie stained Art v 3 and Pru p 3. (B,C) Amino acid distribution determined by amino acid analysis. (D) Intact mass spectrometry analyses.

pH 3.4 or pH 7.3. Protein samples were heated at 95 °C for up to 120 min (Stock et al., 2018). Based on the determined isolectric point for Art v 3 (p*I* 8.80) and Pru p 3 (p*I* 9.25), the net charge at the acidic pH is strongly positive due to protonation.

2.6. Circular dichroism and FTIR

Circular dichroism (CD) and thermal denaturation were recorded in 10 mM sodium phosphate pH 7.3 or pH 3.4 using a JASCO J-815 spectropolarimeter (Jasco, Tokyo, Japan). Far UV-spectra (190–260 nm) were recorded at 20 °C, 95 °C and 20 °C after renaturation in the CD cuvette. In addition, spectra of heat treated samples were monitored at 20 °C and results are presented as mean residue molar ellipticity. Secondary structure predictions were performed with the online tool K2D3 (Louis-Jeune et al., 2012). Infrared spectra were recorded at 1.5 mg/ml at 25 °C using a Tensor II Confocheck FTIR system (Bruker Optics Inc., Billerica, MA, USA) in the range of 3100-1000 cm^{-1}, details of the procedure are given online.

2.7. Dynamic light scattering and size exclusion chromatography

Aggregation behaviour of the differently treated samples of Art v 3 and Pru p 3 were investigated by dynamic light scattering (DLS 802, Viscotek Corp., Houston, TX, USA). Data were accumulated for 10 x 5 s and the correlation function was fitted into the combined data curve from which the intensity distribution was calculated. The hydrodynamic radius and estimated molecular mass of proteins were calculated with the provided software. SEC-UV was performed on an UltiMate® 3000 (Thermo Fisher Scientific, MA, USA) equipped with an Acclaim™ SEC-300 pre-column (4.6 x 33 mm; 5 µm particle size; 300 Å pore size) and an Acclaim™ SEC-300 column (4.6 x 300 mm; 5 µm particle size; 300 Å pore size), both from Thermo Fisher Scientific (Waltham, MA, USA). Details on the settings can be found in the online repository.

2.8. Determination of lanthionine formation

Upon thermal treatment of Art v 3 and Pru p 3, the formation of lanthionine bonds was analyzed by peptide mass fingerprinting. Proteolytic digestion of 2 µg was performed upon addition of 1:10 (*w/w*) trypsin (porcine pancreas, mass spec grade, Promega, Madison, WI, USA) for 3 h at 37 °C after prior reduction and alkylation of disulfides. Obtained peptides were separated employing reversed-phase HPLC on an UltiMate® 3000 Rapid Separation system equipped with a Hypersil Gold aQ C18 column. Mass spectrometry was performed using a Thermo Scientific Q Exactive™ Plus benchtop quadrupole-Orbitrap mass spectrometer. Detailed settings can be found online.

2.9. IgG and IgE ELISA

The IgG-binding activity of heated and non-heated Art v 3 and Pru p 3 was investigated in ELISA using a serum pool from mice (n = 6) previously immunized with Art v 3 or Pru p 3 (Gadermaier et al., 2011a). In addition, sera from 26 Italian patients presenting inhalation and/or ingestion related allergy symptoms to LTP containing pollen or food sources with a positive IgE result to Art v 3 and Pru p 3 on ImmunoCAP ISAC (Thermo Fisher Scientific, Uppsala, Sweden) were included in this study. Demographic details, clinical symptoms and IgE sensitization determined by ImmunoCAP ISAC are provided in Online Table 2. The study was approved by the Institutional Review Board (n. 106-CE-2005). For ELISA, purified non-treated and heated proteins were coated overnight at 4 °C to ELISA plates. After washing and blocking steps as described in detail in the online section, plates were incubated with a serial dilutions of the murine serum pool or 1:5 diluted patients' serum. Alkaline phosphatase conjugated rabbit anti-mouse IgG/IgM or monoclonal mouse anti-human IgE antibodies were used as secondary antibody. 4-Nitrophenyl-phosphate was used as substrate and optical density was measured at 405 nm.

2.10. Statistical analyses

Statistical analyses were performed in GraphPad Prism 7.03. For ELISA, a Spearman correlation of the IgE reactivities was performed and the correlation coefficient (r) is given. In addition, a Friedman test followed by Dunn's multiple comparison post-hoc test was performed.

3. Results

3.1. Production and physicochemical characterization of Art v 3 and Pru p 3

Art v 3.0201 and Pru p 3.0102 were obtained under analogous production conditions as non-fusion proteins in *E. coli*. Recombinant proteins were purified by cation exchange chromatography to > 98% purity and a yield of 4.5 mg (Art v 3) and 3.0 mg (Pru p 3) per liter bacterial culture, respectively (Fig. 1A). Exact concentrations were obtained by amino acid analysis and residue distributions were in good agreement with theoretical values (Fig. 1B,C). The experimentally determined mass of intact allergens under non-reducing conditions was in excellent agreement with the theoretical value (Fig. 1D), and revealed that all eight cysteine residues were involved in disulfide bond formation. CD spectra presented minima at 222 and 208 nm and a maximum at 193 nm indicative of an alpha helical fold (Online Fig. E1). Upon heating to 95 °C in the CD cuvette, proteins showed an overall decrease in spectra signals. After subsequent cooling to 20 °C, both proteins were able to refold under acidic conditions while in contrast spectra at neutral pH were identical with those obtained at 95 °C.

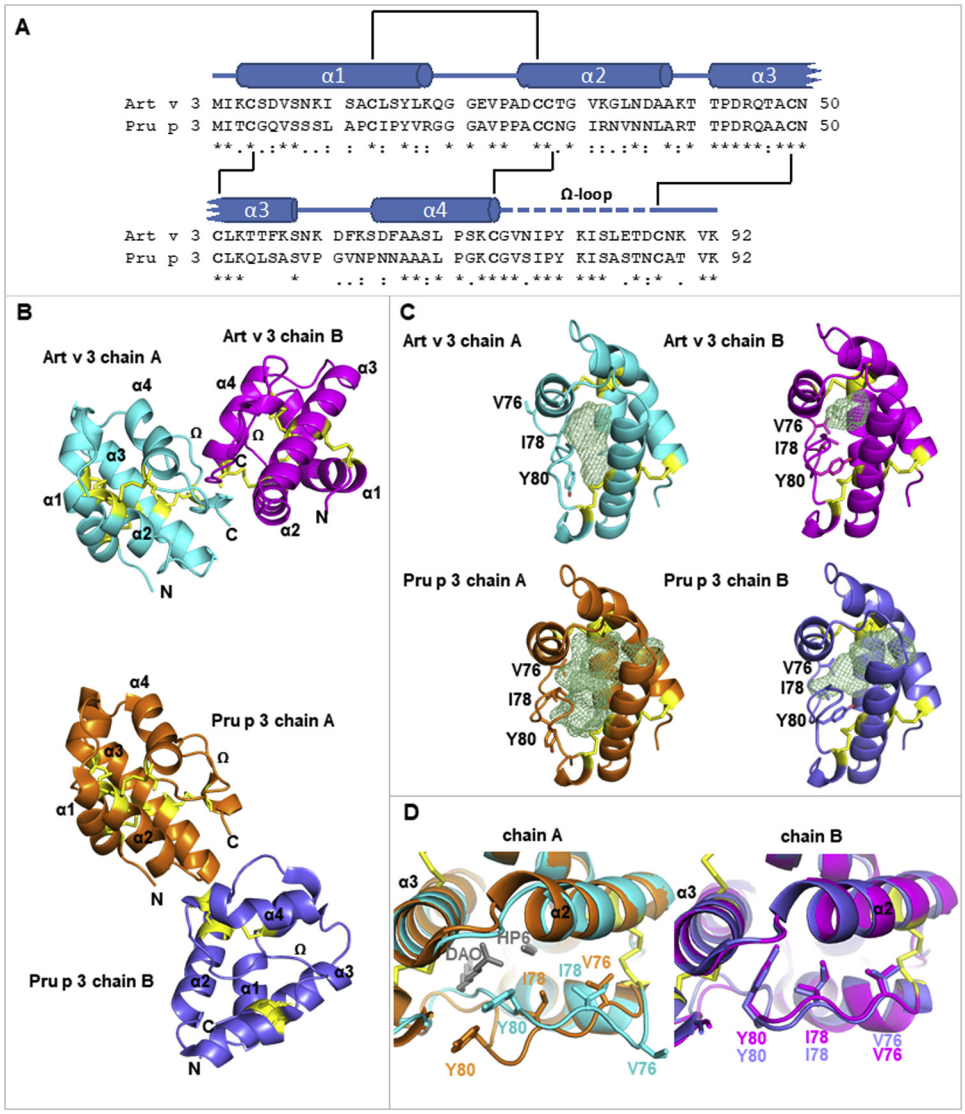

Fig. 2. X-ray crystallography of Art v 3 and comparison to Pru p 3. (A) Sequence alignment of Art v 3 and Pru p 3 generated by CLUSTAL O 1.2.4; asterisks (*) indicate identical residues, colons (:) indicate strongly similar residues, periods (.) indicate weakly similar residues. Black lines indicate disulfide bonds and the dashed line represents the Ω loop. (B) The crystallographic asymmetric units of Art v 3 (PDB 6FRR) and Pru p 3 (PDB 2ALG) contain two molecules each, interacting asymmetrically at different interfaces. (C) The ligand-binding cavity is depicted as green mesh and the differences in cavity volume reflect the adaptive nature of the proteins. The pockets were calculated using POCASA (version 1.1) web server (Yu et al., 2010). (D) Close view of the aligned Ω loop region of Art v 3 and Pru p 3 chain A and B. Hydrophobic residues V76, I78 and Y80 formed a lid to the hydrophobic cavity, thereby reducing the cavity volume (For interpretation of the references to colour in this figure legend, the reader is referred to the web version of this article.).

3.2. Crystal structure of Art v 3 and comparison to Pru p 3

As the structure of Art v 3 was unknown, we first solved the 3-D structure by X-ray crystallography to 1.9 Å (PDB: 6FRR). The stability of the structure depends on the presence of four intramolecular disulfide bonds determined at C4-C51, C14-C28, C29-C74 and C49-C88 (Fig. 2A,B). Despite only 51% identity at the amino acid level, the previously published structure of Pru p 3 (PDB: 2ALG) presents an overall similar fold and was used for comparison. Under the given crystallization conditions, Art v 3 presented two independent molecules in the asymmetric unit, each molecule organized as antiparallel four helix bundle (M1-C74) with a C-terminal extension that was not secondarily structured (G75-K92). Both, Art v 3 and Pru p 3 crystals contain two molecules in the asymmetric unit, while the protein contacts are different (Fig. 2B). When structurally aligning Art v 3 and Pru p 3, the potential ligand entry site between alpha 1 and 3 were positioned similarly. The observed differences in the lipid binding cavities at (the entrance to) the ligand binding pockets result from cumulative changes in side chain and loop positions rather than a pronounced change in the secondary structure elements (Fig. 2C). Additionally, the flexible Ω loop (G75-D87, numbering based on Art v 3) significantly influenced the volume of the binding pocket. Notably, the differences in the Ω-loop were more pronounced between the two chains in Art v 3 as compared to Pru p 3. The three hydrophobic residues V76, I78 and Y80 formed a lid to the hydrophobic cavity thereby reducing the cavity volume; changes like flipping of Y80 and V76 are necessary to generate a larger cavity volume for accommodation of ligands (Fig. 2D).

3.3. Effects of heating on secondary structure elements

To investigate the influence of thermal stress conditions on intrinsic features of LTPs, Art v 3 and Pru p 3 were in parallel heated at 95 °C under acidic (pH 3.4) and neutral (pH 7.3) conditions for 0, 5, 15, and 120 min. CD spectra of native proteins revealed identical spectra for either protein at pH 3.4 and 7.3, respectively, indicative of alpha helical structures at both pH conditions (Fig. 3). At acidic pH, Art v 3 was more susceptible to denaturation as observed in the 15 min denatured sample, while the spectra of Pru p 3 was only affected after 120 min treatment (Fig. 3A,B). Treatment at neutral conditions induced random coil structures indicated by the negative amplitude around 195–200 nm (Fig. 3C,D). Art v 3 is more stable under neutral conditions, as loss of the alpha helical structure is only observed in the 120 min treatment sample while random coil structures are detectable in the 15 min denaturation sample of Pru p 3. Secondary structure predictions using the online tool K2D3 revealed a loss of alpha helices at prolonged thermal treatment at acidic pH with higher susceptibility of Art v 3. At neutral conditions, a substantial loss of alpha helices was noted already after 5 min which extended to < 6.6% at 120 min. While the vast majority of

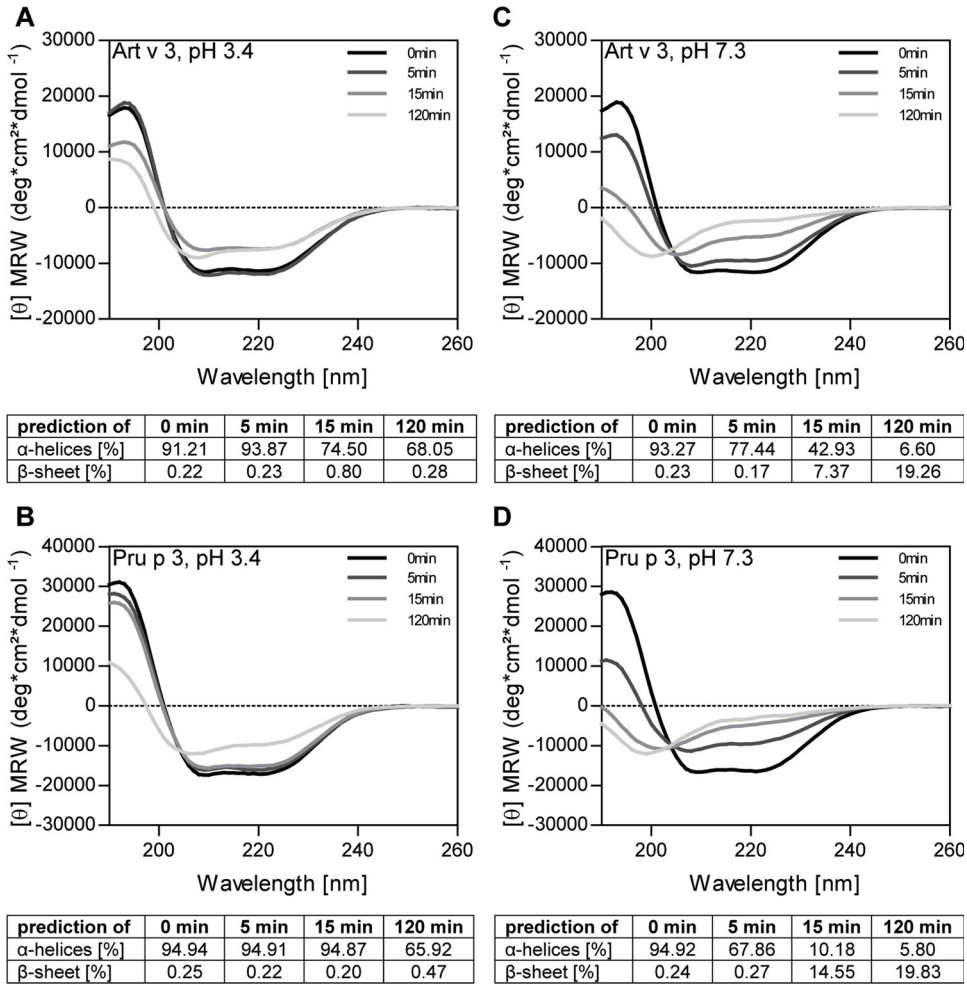

prediction of	0 min	5 min	15 min	120 min
α-helices [%]	91.21	93.87	74.50	68.05
β-sheet [%]	0.22	0.23	0.80	0.28

prediction of	0 min	5 min	15 min	120 min
α-helices [%]	93.27	77.44	42.93	6.60
β-sheet [%]	0.23	0.17	7.37	19.26

prediction of	0 min	5 min	15 min	120 min
α-helices [%]	94.94	94.91	94.87	65.92
β-sheet [%]	0.25	0.22	0.20	0.47

prediction of	0 min	5 min	15 min	120 min
α-helices [%]	94.92	67.86	10.18	5.80
β-sheet [%]	0.24	0.27	14.55	19.83

Fig. 3. Circular dichroism spectra of thermally treated LTPs and secondary structure predictions of Art v 3 and Pru p 3.

the protein appeared disordered, concomitant induction of beta sheets up to 19% was suggested by the online prediction tool (Fig. 3).

Additionally, FTIR measurements of the native and 120 min heat treated proteins were performed and depicted as the second derivative spectra of the amide I region at 1700-1600 cm^{-1} (Fig. 4). The spectra of both native proteins showed a negative peak around 1655 cm^{-1} under both pH conditions which can be assigned to alpha helices. While the spectrum of heat-treated Art v 3 at pH 3.4 was similar to the native, Pru p 3 alpha helical signals decreased and an additional signal around 1644 cm^{-1} was revealed (Fig. 4A,B). Upon heating at neutral pH, both proteins showed slightly increased signals around 1680 cm^{-1} and 1640 cm^{-1} indicative of β-sheets/turns and β-sheets, respectively. Similar to CD, changes in spectra were typically more pronounced for Pru p 3 except for the β-sheet region.

3.4. Effects of heating on protein conformation and aggregation

The aggregation behavior of heat-treated proteins was monitored by DLS and SEC. A hydrodynamic radius (R_H) of 1.8 nm (~13 kDa) was determined for native Art v 3, indicating a monomeric molecule (Fig. 5A). The R_H of Pru p 3 is lower presenting only 1.5 nm, translating to a molecular mass of ~9 kDa. Heat treatment under acidic conditions did not lead to significant changes for Art v 3 while minor differences in peak shape of Pru p 3 were observed. In contrast, both molecules showed a significant increase in R_H upon heating at neutral pH. While for Art v 3 this effect was noticeable after 15 min, Pru p 3 already showed a gradual increase in size after 5 min of treatment (Fig. 5A). Upon treatment for 120 min, Art v 3 showed a hydrodynamic radius of 2.3 nm (~24 kDa) and Pru p 3 presented with 2.1 nm (~19 kDa).

To analyze if the observed R_H increase is due to dimerization or multimerization, SEC experiments were carried out (Online Fig. E2). The retention time of native Art v 3 was 8.6 min, translating to a calculated mass of 10 kDa. After 120 min heating at acidic conditions, the peak height decreased while the retention time was the same. At neutral conditions, heat treatment showed a retention time of 8.4 min indicating a slight increase in the R_H corresponding to a 12–13 kDa protein (Online Fig. E2A). Retention time of native Pru p 3 was 9.3 min (~5 kDa) suggesting a considerable smaller protein compared to Art v 3. While treatment at acidic conditions did not lead to significant changes, heating for 120 min at neutral conditions presented an elution time of 8.7 corresponding to an increased mass of ~9 kDa (Online Fig. E2B).

3.5. Effects of heating on disulfide bond disruptions and lanthionine formations

Since observed changes in the hydrodynamic radius do not result from multimerization, we focused on cysteine bond rearrangement by non-reversible lanthionine formation as described for Art v 3 recently (Stock et al., 2018). Of note, untreated Art v 3 and Pru p 3 were devoid of lanthionine formations. Heat-treated Art v 3 presented numerous different peptides involving lanthionine bonds, which were mostly detectable after 120 min heating at neutral conditions (pH 7.3), whereas under acidic conditions (pH 3.4) lanthionine formation was hardly observed (Online Fig. E3). It seems that especially lanthionine C28-C29 is involved in a rather early onset of this irreversible modification;

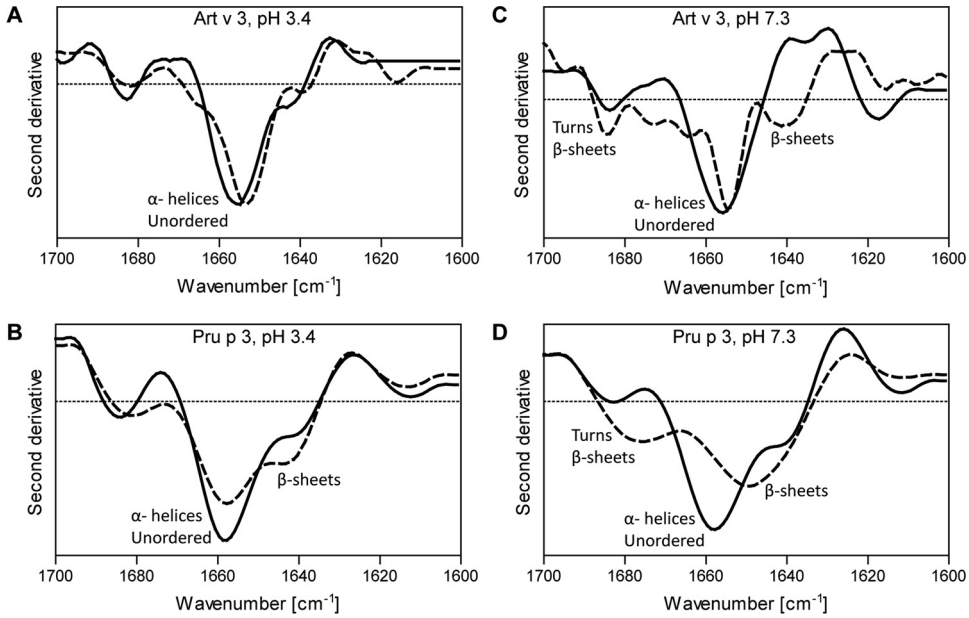

Fig. 4. Secondary structure analysis using FTIR. Second derivatives in the amide I region of the FTIR absorbance spectra of thermally treated LTPs. Continuous lines indicate non-treated samples and dotted lines represent samples after 120 min heating at 95 °C.

alternative linkages of C28 and C29 with C49 and C51, respectively, were also observed, albeit on a somewhat slower time scale (Fig. 5B). Other prominent lanthionine formations involve C4-C14 and C74-C88. Regarding Pru p 3, similar observations were made with the exception of only minor appearance of C28/C29-C49/C51 peptides during the course of the experiment (Fig. 5F). Notably, lanthionine formation cannot generally be predicted from the native structure, as structural disruptions precede the lanthionine formations as illustrated for Art v 3 (Fig. 5C).

3.6. Effects of heating on IgG- and IgE-binding epitopes

The influence of heat treatment regarding IgG and IgE binding epitopes of Art v 3 and Pru p 3 was analyzed by ELISA. Using serial dilutions of sera from Art v 3 or Pru p 3 immunized mice, no significant differences in reactivity were observed for the native proteins in different buffers (Fig. 6 A,B). Heat treatment at acidic conditions did not influence antibody binding to Art v 3 while a slight decrease in reactivity towards Pru p 3 was noted. At neutral conditions, a strong time-dependent decrease in IgG binding was observed which was more pronounced for Pru p 3, leading to an abrogated antibody reactivity after 120 min for both allergens.

In addition, IgE reactivity of 26 LTP-allergic patients' sera was evaluated (Fig. 6 C,D). IgE binding capacity of the native proteins at acidic and neutral pH was perfectly correlating for Art v 3 ($r = 0.9913$) and Pru p 3 ($r = 0.9891$), respectively. Heat treatment of proteins at acidic conditions showed a moderate but statistically significant reduction for Art v 3 starting from 15 min treatment ($p = 0.0066$) while no changes were observed for Pru p 3. Heating at neutral pH led to a drastic reduction in IgE binding towards both proteins. A difference in the kinetics was though revealed when analyzing the 15 min treated sample. While IgE reactivity of Art v 3 was decreased by 30% ($p = 0.0018$), only an 11% reduction which was statistically not significant was observed for Pru p 3. After 120 min heating at pH 7.3, the IgE binding capacity was abrogated with the exception of one patient remaining clearly positive to Pru p 3 (Fig. 6 C,D).

4. Discussion

Within this study, we investigated the structural and immunological features of clinically relevant non-specific LTPs (Asero et al., 2018; Basagana et al., 2018; Sanchez-Lopez et al., 2014) using prototypic family members from pollen (Art v 3 from mugwort) and food (Pru p 3 from peach). Due to their compact fold, LTPs exhibit high stability to thermal treatment and proteolytic digestion which can lead to allergic reactions towards processed (food) sources (Duffort et al., 2002; Brenna et al., 2000; Sancho et al., 2005). It was previously shown that heat treatment in different buffer environments has varying impact on their secondary structure (Gaier et al., 2008; Gadermaier et al., 2009, 2011b; Vejvar et al., 2013). However, detailed and systematic analysis of structural changes especially upon heating for extended periods with concomitant immunological investigations is not available.

The 3-dimensional structure of some allergenic and non-allergenic food LTPs has been solved (Pasquato et al., 2006; Shenkarev et al., 2017; Bogdanov et al., 2016; Melnikova et al., 2016; Bakan et al., 2009; Offermann et al., 2015; Cheng et al., 2004; Jain and Salunke, 2017), while so far no LTP originating from pollen has been addressed. Within this work, we solved the first 3-D structure of a pollen LTP showing the typical cysteine-stabilized alpha helical fold. Similar to other LTPs (Pasquato et al., 2006; Bakan et al., 2009; Shenkarev et al., 2017; Bogdanov et al., 2016; Melnikova et al., 2016; Bakan et al., 2009; Offermann et al., 2015; Cheng et al., 2004; Jain and Salunke, 2017), Art v 3 was found as dimer in the asymmetric unit. The fact that two molecules were observed in the asymmetric unit does not indicate any tendency for dimerization but rather reflects an intrinsic variability of e.g. Art v 3 and Pru p 3, leading to the crystallization of two different protein conformations. In vitro, LTPs are able to adopt a variety of lipid ligands in their hydrophobic cavity and recently the natural ligand of Pru p 3 was identified as a derivative of camptothecin binding to phytosphingosine (Scheurer and Schulke, 2018; Cubells-Baeza et al., 2017; Dubiela et al., 2017, 2019). It is noteworthy to mention that the published structure of Pru p 3 (PDB: 2ALG) was obtained upon *Pichia pastoris* expression and crystalized in the presence of cargo molecules (Pasquato et al., 2006). In specific, chain A was loaded with two ligands, i.e. lauric acid and heptane, chain B was half-loaded with lauric acid with the lipid tail being inside and carbonyl group sticking out of the protein. Based on this observation, one can speculate that one of the potential ligand entry sites is between alpha 1 and 3 (Fig. 2B), where a lipophilic ligand was bound in the Pru p 3 chain B. By contrast, Art v 3 was crystalized in an unloaded (apo)-form in our study. Interestingly,

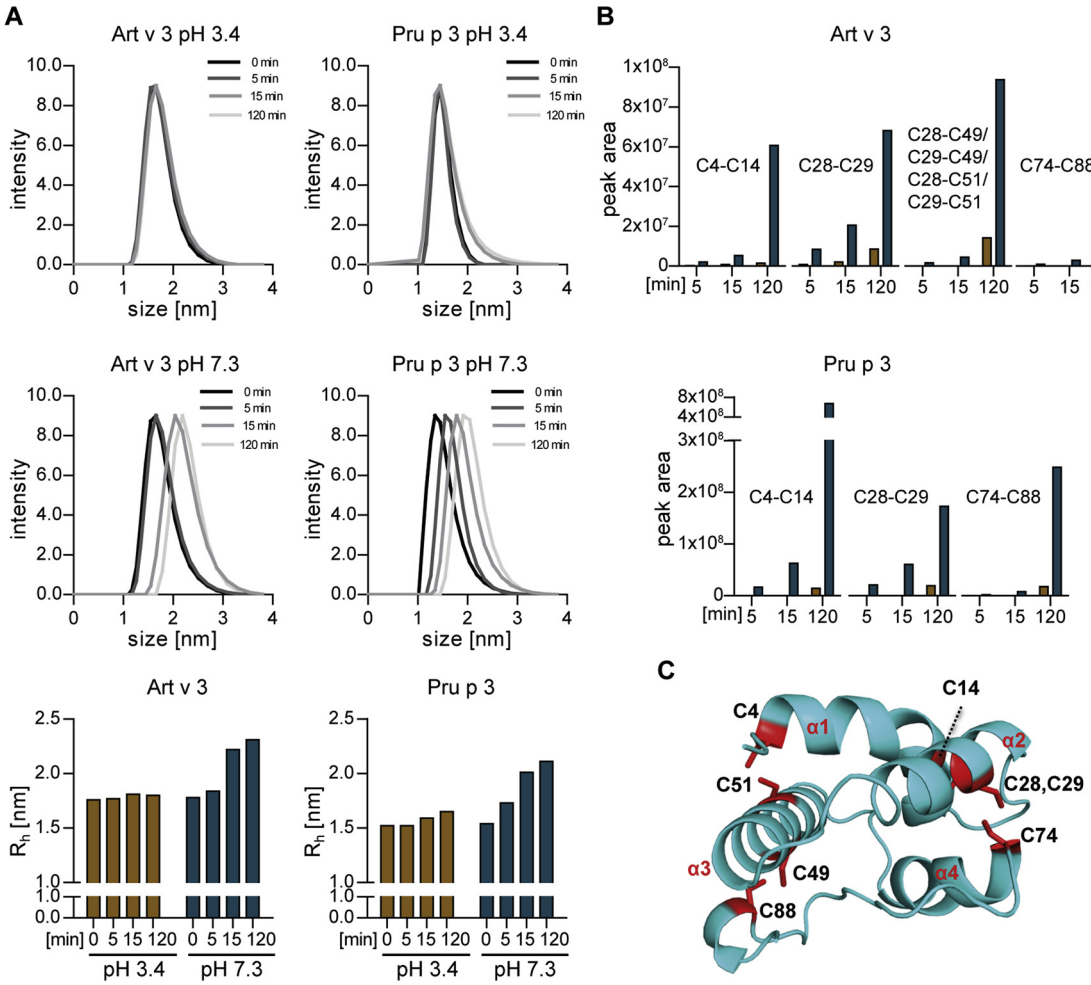

Fig. 5. Dynamic light scattering and detection of lanthionine containing peptides. (A) The aggregation status and hydrodynamic radius of thermally treated LTPs were monitored by dynamic light scattering. (B) Semi-quantitative mass-spectrometry based analysis of lanthionine containing peptides upon time dependent treatment at pH 3.4 (beige bars) and pH 7.3 (cyan bars). Lanthionine containing peptides with highest peak areas are depicted here; detailed graphics of all identified lanthionine containing peptides is provided in Supplementary Fig. 3). (C) For Art v 3, suggested early lanthionine formation of C28-C29 initiates linkage of C4-C14 and C74-C88 leading to structural disruption of the LTP fold. All cysteine residues are colored in red (For interpretation of the references to colour in this figure legend, the reader is referred to the web version of this article.).

while the cartoon representations emphasizing the secondary structure elements to appear very similar in the studied molecules, the dimensions of their binding pockets vary strongly. This indicates that the pocket load as well as protein contacts influence the conformation more than variations in the amino acid sequence difference of around 50%. Consistent with this analysis, the conformational flexibility in the Ω loop region was shown by a high crystallographic B-factor and an increased local variability as revealed by Pru p 3 molecular dynamics simulations (Pasquato et al., 2006). In one of the two independent chains of the Art v 3 and Pru p 3 crystals (chain B), the three hydrophobic residues V76, I78 and Y80 are pointing into the cavity, thereby forming a lid to the hydrophobic cavity and reducing the internal volume. A similar conformation was observed in the apoform of rice LTP (PDB: 1RZL). The closed conformation would theoretically crash with the ligand DAO present in Pru p 3 chain A. To accommodate for DAO binding, Y80 rotated away from the cavity and the entire Ω loop region was moving away, as shown in Pru p 3 chain A. Despite the absence of a ligand, similar large movements were observed for chain A of Art v 3, where Y80 and V76 were flipped out of the cavity and I78 was shifted to the position of V76, thereby expanding the size of the cavity. These structural variations show that the Ω loop can adopt different conformations thereby changing the cavity volume and thus encodes an adaptation element to accommodate different ligands with relevance to its physiological function.

In previous CD experiments, differences regarding structural susceptibility upon heat treatment of LTP in acidic and neutral environment were revealed (Gadermaier et al., 2011a; Gaier et al., 2008; Gadermaier et al., 2011b; Vejvar et al., 2013; Johnson et al., 2010). Typically, denaturation at neutral or slightly alkaline pH led to irreversible structural alterations, while Mal d 3 from apple was shown to refold when the protein was heated in the absence of oxygen (Sancho et al., 2005). Those studies prompted us to investigate this phenomenon in more detail assessing for the first time structural changes of unloaded Art v 3 and Pru p 3 in a holistic and time-dependent manner. To verify intrinsic features, allergens were expressed as non-fusion proteins in *E. coli* and formation of disulfide bonds was enabled using the Rosetta-gami strain (Gadermaier et al., 2009, 2011b). To justify physicochemical and immunological comparison, proteins were produced and purified under identical conditions. Highly pure recombinant proteins were obtained and identity was verified by amino acid analysis and mass spectrometry. The alpha helical fold was monitored in CD spectroscopy as well as FTIR (Gaier et al., 2008; Gadermaier et al., 2009; Rigby et al., 2008). Though both molecules are similar in mass, Pru p 3 consistently appeared more compact in DLS and SEC experiment. This observation is most likely due to the more extensive hydration shell for Art v 3 which can be explained by the different composition of charged amino acids.

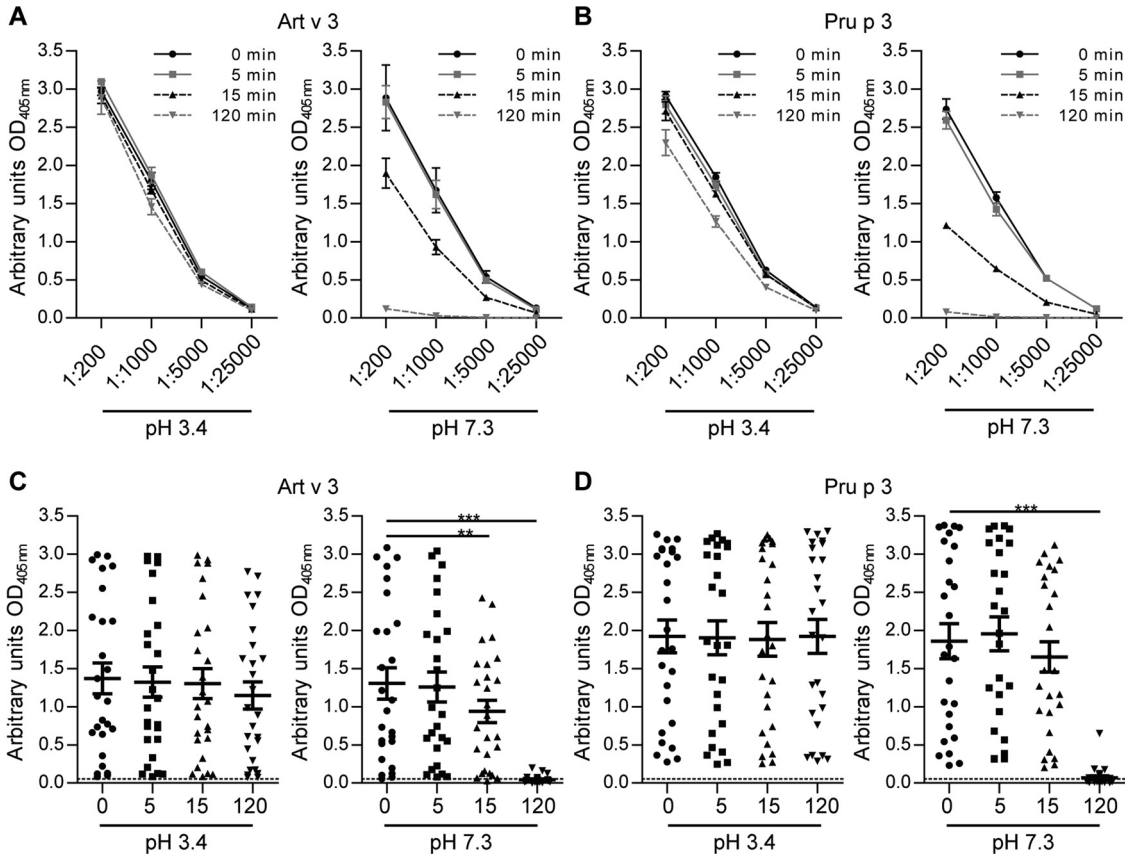

Fig. 6. Antibody binding analyses to thermally treated LTPs using ELISA. (A,B) IgG binding in serial dilutions was investigated using a serum pool of mice (n = 6) immunized with Art v 3 (A) or Pru p 3 (B). (C, D) IgE binding was investigated using 26 LTP allergic patients' sera. Dotted lines represent ELISA thresholds, black lines indicate mean values and ± SEM. Data were statistically analyzed by a Friedman test followed by Dunn's multiple comparison post-test against the 0 min sample. *** $p \leq 0.001$, ** $p \leq 0.01$.

Art v 3 contains 23 charged residues (14 basic and 9 acidic amino acids), whereas the number of charged residues for Pru p 3 is only 9 (8 basic and 1 acidic amino acid). In fact, the percentage of charged compared to total surface areas is 30% for Art v 3 while it is only 14% for Pru p 3.

At acidic conditions, both proteins were highly stable and extensively heat-treated samples mostly demonstrated a minor decrease in peak height while at the same time peak broadening was observed in SEC. No relaxation of the compact LTP fold was observable for Art v 3 in DLS and SEC, while Pru p 3 did present a slightly enlarged R_H. While previous studies mostly focused on CD denaturation and renaturation (Gaier et al., 2008; Gadermaier et al., 2009, 2011b; Rigby et al., 2008), this is the first to additionally assess differences upon extensive heating using FTIR, a method providing an even closer insight. Generally, loss of alpha helices and induction of disordered structures was observed for both molecules, while neutral conditions additionally favored generation of some beta-sheets and turns. The observed spontaneous refolding capacities under acidic conditions can be rationalized by the disulfide-bond stabilized secondary structures where alpha helices can fold locally as disulfide shuffling is mostly suppressed at low pH (Rombouts et al., 2015; Thing et al., 2010).

In contrast, thermal treatment at neutral pH drastically influenced the structure with Pru p 3 being more prone to secondary structure changes compared to Art v 3. Both molecules showed an increase in R_H indicating a relaxation of the compact LTP fold. Based on the gradual increase in the observed molecule size and only a minor shift in retention time in SEC, it seems that proteins undergo structural rearrangements rather than dimerization or oligomerization (Sancho et al., 2005). While both molecules presented a random coil spectrum after extensive heat treatment, Pru p 3 lost its structural integrity already after 15 min heating. Both, CD secondary prediction and FTIR measurements indicate tremendous decrease of α-helices and interestingly a minor induction of β-sheets. Though formation of β-sheets was suggested to be related with protein aggregation (Koppelman et al., 1999), results from SEC experiments do not support this hypothesis for the investigated molecules.

Irreversible conformational changes at neutral to basic pH have been related to thermally induced disulfide-bond shuffling, where new intermolecular cysteine-linkages are generated after disulfide bond cleavage by β-elimination. This reaction can lead to the formation of stable aggregates, which was previously observed for bovine α-lactalbumin, thaumatin and transferrin (Gaier et al., 2008; Wijesinha-Bettoni et al., 2007; Kaneko and Kitabatake, 1999). Another possible reaction is the formation of thioether bonds due to disulfide bond cleavage. Intramolecular disulfide bonds can be cleaved by β-elimination reactions upon heating at high temperatures and alkaline pH. This leads to the generation of dehydroalanines and free cysteines which can further react to form the irreversible cross-link lanthionine (Galande et al., 2003; Lu and Chang, 2010). Lanthionine formation was shown to be protein specific and depends on the proximity between alkaline amino acids and free cysteines (Bar-Or et al., 2008; Rombouts et al., 2016). Indeed, we could recently demonstrate by CZE-ESI-MS that irreversible conformational changes of thermally treated Art v 3 are mainly due to lanthionine formation and identified some lanthionine positions including transiently formed trisulfide bonds. Those lanthionine variants showed higher charge states in MS suggesting different conformations in agreement with the enlargement of molecules shown within this study (Stock et al., 2018). Of note is the fact, that Art v 3 presents 14 basic amino acids, while Pru p 3 contains 8 alkaline residues, with some in close vicinity to cysteine residues.

Based on the kinetics and semi-quantitative amount of lanthionine containing peptides, initial formation of lanthionines seems to take place between C28-C29 which must be preceded by the disruption of the two original disulfide bonds C14-C28 and C29-C74. Interestingly, C14 and C74 preferably linked as lanthionine C4-C14 and C74-C88 involving the most N- as well as C-terminal cysteine residues; the terminal protein segments are typically the most flexible, thus sterically enabling the lanthionine reactions. Other linkages between C28/C29-C49/C51 were frequently observed which however cannot be exactly localized due to the fact that two different cysteines each co-localize in the respective peptides analyzed by MS. Although quantitatively most prevalent, suggested arrangements are not mutually exclusive and different Art v 3 populations with slightly different lanthionine profiles are simultaneously observed in capillary electrophoresis (Stock et al., 2018). Lanthionine formation of Pru p 3 generally followed the same pattern but lacked the interaction C28/C29-C49/C51 which was rather prominent in Art v 3. Formation of novel non-reversible lanthionines was certainly accompanied by structural disruption of the molecules as represented in data from CD and FTIR measurements. Elucidation of lanthionine establishment upon heat treatment of LTPs represents a first step to better understand structural changes in cysteine-bond stabilized molecules. So far, generation of hypoallergens for allergen specific immunotherapy proved to be extremely challenging when targeting disulfide bond stabilized molecules (Jongejan et al., 2016; Toda et al., 2011; Eichhorn et al., 2019). New insights provided in this study might help to better understand and thus rationally design such hypoallergenic variants of relevant allergens from e.g. peach, peanut and pellitory pollen.

In ELISA experiments using sera from mice and LTP-allergic patients, antibody binding was largely unaffected upon thermal treatment at acidic pH. These results are consistent with previous studies showing that thermally processed LTP-containing foods like peach juice (Brenna et al., 2000; Garino et al., 2012), cooked apples (Sancho et al., 2005; Asero et al., 2003), polenta (Pastorello et al., 2003) and cooked cherries (Scheurer et al., 2004) are still able to elicit allergic reactions. On the other hand, IgG and IgE binding to both proteins was completely abrogated after 120 min heating at neutral conditions. This strongly points at conformational epitopes, which were disintegrated upon irreversible cysteine bond rearrangement due to lanthionine formation. While Pru p 3 seems to unfold earlier and thus cause a faster loss of IgG reactivity, IgE epitopes seem to be fairly intact in the 15 min heat-treated sample. It generally seems that investigated epitopes are only partially overlapping and several studies reported that Pru p 3 possesses more IgE epitopes which might explain the observation (Egger et al., 2010). However, while IgE epitopes of peach, wheat and pellitory pollen LTP have been identified using peptides, fragments or mimotopes (Garcia-Casado et al., 2003; Colombo et al., 1998; Longo et al., 2015; Pacios et al., 2008; Tordesillas et al., 2009), further data on conformational IgE epitopes are largely missing for the LTP protein family. Within our study, antibody reactivity of Art v 3 and Pru p 3 was clearly disrupted upon extensive heating at neutral conditions, suggesting the formation of novel structures that neither represent original conformational antibody binding sites nor reflects regions present in linear epitopes. Our findings have direct implications for processing of LTP-containing food products, as allergenic epitopes might be destroyed but conversely also still exist after heat-treatment depending on the pH of the product matrix. As a result, the treatment procedure defines if predisposed individuals will be confronted with allergic reactions to the sensitized food and possibly other LTP-containing food sources as a consequence of IgE cross-reactivity.

Within this study, we solved the crystal structure of Art v 3 from mugwort pollen and compared it with the prototypic LTP family member Pru p 3. Upon extensive heating in acidic buffer, both recombinant allergens were highly stable and presented only minor changes in conformation and antibody binding. In contrast, thermal treatment in neutral conditions led to irreversible structural changes and cysteine bond rearrangements due to lanthionine formations. Despite the overall similarity, the structural integrity of the more compact Pru p 3 molecule was earlier affected which did however only partially influence IgE binding epitopes. Based on our results, it is crucial to consider the buffer environment and duration when thermally processing LTP containing foods or food products as this will highly influence the structure and consequently potential allergic (cross)-reactions.

Funding

The financial support by the Austrian Federal Ministry for Digital and Economic Affairs, the National Foundation for Research FWF (project W_01213), Technology and Development and a startup grant from Land Salzburg is gratefully acknowledged. The funding sources had no involvement in study design, data analysis and writing of the manuscript.

Declaration of Competing Interest

Novartis and Thermo Fisher Scientific GmbH provide financial support for the Christian Doppler Laboratory for Innovative Tools for Biosimilar Characterization, Salzburg, Austria. The salary of S.W. and L.G.S. was fully funded, C.G.H.'s salary is partly funded by the Christian Doppler Laboratory for Biosimilar Characterization. The other authors declare no conflict of interest.

Acknowledgement

We would like to thank Fatima Ferreira and Mario Schubert for scientific discussions and Ronald van Ree and Serge Versteeg for providing the Pru p 3 plasmid construct.

Appendix A. Supplementary data

Supplementary material related to this article can be found, in the online version, at doi:https://doi.org/10.1016/j.molimm.2019.10.012.

References

Afonine, P.V., Grosse-Kunstleve, R.W., Echols, N., Headd, J.J., Moriarty, N.W., Mustyakimov, M., Terwilliger, T.C., Urzhumtsev, A., Zwart, P.H., Adams, P.D., 2012. Towards automated crystallographic structure refinement with phenix.refine. Acta Crystallogr. D Biol. Crystallogr. 68, 352–367.

Asero, R., Piantanida, M., Pinter, E., Pravettoni, V., 2018. The clinical relevance of lipid transfer protein. Clin. Exp. Allergy 48, 6–12.

Asero, R., Mistrello, G., Roncarolo, D., de Vries, S.C., Gautier, M.F., Ciurana, C.L., Verbeek, E., Mohammadi, T., Knul-Brettlova, V., Akkerdaas, J.H., Bulder, I., Aalberse, R.C., van Ree, R., 2001. Lipid transfer protein: a pan-allergen in plant-derived foods that is highly resistant to pepsin digestion. Int. Arch. Allergy Immunol. 124, 67–69.

Asero, R., Mistrello, G., Roncarolo, D., Amato, S., Falagiani, P., 2003. Analysis of the heat stability of lipid transfer protein from apple. J. Allergy Clin. Immunol. 112, 1009–1011.

Bakan, B., Hamberg, M., Larue, V., Prange, T., Marion, D., Lascombe, M.B., 2009. The crystal structure of oxylipin-conjugated barley LTP1 highlights the unique plasticity of the hydrophobic cavity of these plant lipid-binding proteins. Biochem. Biophys. Res. Commun. 390, 780–785.

Barber, D., de la Torre, F., Feo, F., Florido, F., Guardia, P., Moreno, C., Quiralte, J., Lombardero, M., Villalba, M., Salcedo, G., Rodriguez, R., 2008. Understanding patient sensitization profiles in complex pollen areas: a molecular epidemiological study. Allergy 63, 1550–1558.

Bar-Or, R., Rael, L.T., Bar-Or, D., 2008. Dehydroalanine derived from cysteine is a common post-translational modification in human serum albumin. Rapid Commun. Mass Spectrom. 22, 711–716.

Basagana, M., Elduque, C., Teniente-Serra, A., Casas, I., Roger, A., 2018. Clinical profile of lipid transfer protein syndrome in a Mediterranean Area. J. Investig. Allergol. Clin. Immunol. 28, 58–60.

Bernardi, M.L., Giangrieco, I., Camardella, L., Ferrara, R., Palazzo, P., Panico, M.R., Crescenzo, R., Carratore, V., Zennaro, D., Liso, M., Santoro, M., Zuzzi, S., Tamburrini, M., Ciardiello, M.A., Mari, A., 2011. Allergenic lipid transfer proteins from plant-derived foods do not immunologically and clinically behave homogeneously: the kiwifruit LTP as a model. PLoS One 6, e27856.

Bogdanov, I.V., Shenkarev, Z.O., Finkina, E.I., Melnikova, D.N., Rumynskiy, E.I.,

Arseniev, A.S., Ovchinnikova, T.V., 2016. A novel lipid transfer protein from the pea Pisum sativum: isolation, recombinant expression, solution structure, antifungal activity, lipid binding, and allergenic properties. BMC Plant Biol. 16, 107.
Brenna, O., Pompei, C., Ortolani, C., Pravettoni, V., Farioli, L., Pastorello, E.A., 2000. Technological processes to decrease the allergenicity of peach juice and nectar. J. Agric. Food Chem. 48, 493–497.
Cheng, H.C., Cheng, P.T., Peng, P., Lyu, P.C., Sun, Y.J., 2004. Lipid binding in rice nonspecific lipid transfer protein-1 complexes from Oryza sativa. Protein Sci. 13, 2304–2315.
Colombo, P., Kennedy, D., Ramsdale, T., Costa, M.A., Duro, G., Izzo, V., Salvadori, S., Guerrini, R., Cocchiara, R., Mirisola, M.G., Wood, S., Geraci, D., 1998. Identification of an immunodominant IgE epitope of the Parietaria judaica major allergen. J. Immunol. (Baltimore, Md. : 1950) 160, 2780–2785.
Cubells-Baeza, N., Gomez-Casado, C., Tordesillas, L., Ramirez-Castillejo, C., Garrido-Arandia, M., Gonzalez-Melendi, P., Herrero, M., Pacios, L.F., Diaz-Perales, A., 2017. Identification of the ligand of Pru p 3, a peach LTP. Plant Mol. Biol. 94, 33–44.
Dubiela, P., Aina, R., Polak, D., Geiselhart, S., Humeniuk, P., Bohle, B., Alessandri, S., Del Conte, R., Cantini, F., Borowski, T., Bublin, M., Hoffmann-Sommergruber, K., 2017. Enhanced Pru p 3 IgE-binding activity by selective free fatty acid-interaction. J. Allergy Clin. Immunol. 140 1728-1731 e1710.
Dubiela, P., Del Conte, R., Cantini, F., Borowski, T., Aina, R., Radauer, C., Bublin, M., Hoffmann-Sommergruber, K., Alessandri, S., 2019. Impact of lipid binding on the tertiary structure and allergenic potential of Jug r 3, the non-specific lipid transfer protein from walnut. Sci. Rep. 9, 2007.
Duffort, O.A., Polo, F., Lombardero, M., Diaz-Perales, A., Sanchez-Monge, R., Garcia-Casado, G., Salcedo, G., Barber, D., 2002. Immunoassay to quantify the major peach allergen Pru p 3 in foodstuffs. Differential allergen release and stability under physiological conditions. J. Agric. Food Chem. 50, 7738–7741.
Egger, M., Hauser, M., Mari, A., Ferreira, F., Gadermaier, G., 2010. The role of lipid transfer proteins in allergic diseases. Curr. Allergy Asthma Rep. 10, 326–335.
Eichhorn, S., Horschlager, A., Steiner, M., Laimer, J., Jensen, B.M., Versteeg, S.A., Pablos, I., Briza, P., Jongejan, L., Rigby, N., Asturias, J.A., Portoles, A., Fernandez-Rivas, M., Papadopoulos, N.G., Mari, A., Poulsen, L.K., Lackner, P., van Ree, R., Ferreira, F., Gadermaier, G., 2019. Rational design, structure-activity relationship, and immunogenicity of hypoallergenic Pru p 3 variants. Mol. Nutr. Food Res., e1900336. https://doi.org/10.1002/mnfr.201900336(2019).
Emsley, P., Lohkamp, B., Scott, W.G., Cowtan, K., 2010. Features and development of coot. Acta Crystallogr. D Biol. Crystallogr. 66, 486–501.
Finkina, E.I., Melnikova, D.N., Bogdanov, I.V., Ovchinnikova, T.V., 2016. Lipid transfer proteins As components of the plant innate immune system: structure, functions, and applications. Acta Naturae 8, 47–61.
Gadermaier, G., Harrer, A., Girbl, T., Palazzo, P., Himly, M., Vogel, L., Briza, P., Mari, A., Ferreira, F., 2009. Isoform identification and characterization of Art v 3, the lipid-transfer protein of mugwort pollen. Mol. Immunol. 46, 1919–1924.
Gadermaier, G., Hauser, M., Egger, M., Ferrara, R., Briza, P., Santos, K.S., Zennaro, D., Girbl, T., Zuidmeer-Jongejan, L., Mari, A., Ferreira, F., 2011a. Sensitization prevalence, antibody cross-reactivity and immunogenic peptide profile of Api g 2, the non-specific lipid transfer protein 1 of celery. PLoS One 6, e24150.
Gadermaier, G., Egger, M., Girbl, T., Erler, A., Harrer, A., Vejvar, E., Liso, M., Richter, K., Zuidmeer, L., Mari, A., Ferreira, F., 2011b. Molecular characterization of Api g 2, a novel allergenic member of the lipid-transfer protein 1 family from celery stalks. Mol. Nutr. Food Res. 55, 568–577.
Gaier, S., Marsh, J., Oberhuber, C., Rigby, N.M., Lovegrove, A., Alessandri, S., Briza, P., Radauer, C., Zuidmeer, L., van Ree, R., Hemmer, W., Sancho, A.I., Mills, C., Hoffmann-Sommergruber, K., Shewry, P.R., 2008. Purification and structural stability of the peach allergens Pru p 1 and Pru p 3. Mol. Nutr. Food Res. 52 (Suppl 2), S220–229.
Galande, A.K., Trent, J.O., Spatola, A.F., 2003. Understanding base-assisted desulfurization using a variety of disulfide-bridged peptides. Biopolymers 71, 534–551.
Gao, Z.S., Yang, Z.W., Wu, S.D., Wang, H.Y., Liu, M.L., Mao, W.L., Wang, J., Gadermaier, G., Ferreira, F., Zheng, M., van Ree, R., 2013. Peach allergy in China: a dominant role for mugwort pollen lipid transfer protein as a primary sensitizer. J. Allergy Clin. Immunol. 131, 224–226 e221-223.
Garcia-Casado, G., Pacios, L.F., Diaz-Perales, A., Sanchez-Monge, R., Lombardero, M., Garcia-Selles, F.J., Polo, F., Barber, D., Salcedo, G., 2003. Identification of IgE-binding epitopes of the major peach allergen Pru p 3. J. Allergy Clin. Immunol. 112, 599–605.
Garino, C., Zitelli, F., Travaglia, F., Colsson, J.D., Cravotto, G., Arlorio, M., 2012. Evaluation of the impact of sequential microwave/ultrasound processing on the IgE binding properties of Pru p 3 in treated peach juice. J. Agric. Food Chem. 60, 8755–8762.
Jain, A., Salunke, D.M., 2017. Crystal structure of nonspecific lipid transfer protein from Solanum melongena. Proteins 85, 1820–1830.
Johnson, P.E., Van der Plancken, I., Balasa, A., Husband, F.A., Grauwet, T., Hendrickx, M., Knorr, D., Mills, E.N., Mackie, A.R., 2010. High pressure, thermal and pulsed electric-field-induced structural changes in selected food allergens. Mol. Nutr. Food Res. 54, 1701–1710.
Jongejan, L., van Ree, R., Poulsen, L.K., 2016. Hypoallergenic molecules for subcutaneous immunotherapy. Expert Rev. Clin. Immunol. 12, 5–7.
Kaneko, R., Kitabatake, N., 1999. Heat-induced formation of intermolecular disulfide linkages between thaumatin molecules that do not contain cysteine residues. J. Agric. Food Chem. 47, 4950–4955.
Koppelman, S.J., Bruijnzeel-Koomen, C.A., Hessing, M., de Jongh, H.H., 1999. Heat-induced conformational changes of Ara h 1, a major peanut allergen, do not affect its allergenic properties. J. Biol. Chem. 274, 4770–4777.
Lombardero, M., Garcia-Selles, F.J., Polo, F., Jimeno, L., Chamorro, M.J., Garcia-Casado, G., Sanchez-Monge, R., Diaz-Perales, A., Salcedo, G., Barber, D., 2004. Prevalence of sensitization to Artemisia allergens Art v 1, Art v 3 and Art v 60 kDa. Cross-reactivity among Art v 3 and other relevant lipid-transfer protein allergens. Clin. Exp. Allergy 34, 1415–1421.
Longo, V., Costa, M.A., Cibella, F., Cuttitta, G., La Grutta, S., Colombo, P., 2015. Multiple IgE recognition on the major allergen of the Parietaria pollen Par j 2. Mol. Immunol. 63, 412–419.
Louis-Jeune, C., Andrade-Navarro, M.A., Perez-Iratxeta, C., 2012. Prediction of protein secondary structure from circular dichroism using theoretically derived spectra. Proteins 80, 374–381.
Lu, B.Y., Chang, J.Y., 2010. Rapid and irreversible reduction of protein disulfide bonds. Anal. Biochem. 405, 67–72.
Melnikova, D.N., Mineev, K.S., Finkina, E.I., Arseniev, A.S., Ovchinnikova, T.V., 2016. A novel lipid transfer protein from the dill Anethum graveolens L.: isolation, structure, heterologous expression, and functional characteristics. J. Pept. Sci. 22, 59–66.
Offermann, L.R., Bublin, M., Perdue, M.L., Pfeifer, S., Dubiela, P., Borowski, T., Chruszcz, M., Hoffmann-Sommergruber, K., 2015. Structural and functional characterization of the hazelnut allergen Cor a 8. J. Agric. Food Chem. 63, 9150–9158.
Pacios, L.F., Tordesillas, L., Cuesta-Herranz, J., Compes, E., Sanchez-Monge, R., Palacin, A., Salcedo, G., Diaz-Perales, A., 2008. Mimotope mapping as a complementary strategy to define allergen IgE-epitopes: peach Pru p 3 allergen as a model. Mol. Immunol. 45, 2269–2276.
Palacin, A., Gomez-Casado, C., Rivas, L.A., Aguirre, J., Tordesillas, L., Bartra, J., Blanco, C., Carrillo, T., Cuesta-Herranz, J., de Frutos, C., Alvarez-Eire, G.G., Fernandez, F.J., Gamboa, P., Munoz, R., Sanchez-Monge, R., Sirvent, S., Torres, M.J., Varela-Losada, S., Rodriguez, R., Parro, V., Blanca, M., Salcedo, G., Diaz-Perales, A., 2012. Graph based study of allergen cross-reactivity of plant lipid transfer proteins (LTPs) using microarray in a multicenter study. PLoS One 7, e50799.
Pasquato, N., Berni, R., Folli, C., Folloni, S., Cianci, M., Pantano, S., Helliwell, J.R., Zanotti, G., 2006. Crystal structure of peach Pru p 3, the prototypic member of the family of plant non-specific lipid transfer protein pan-allergens. J. Mol. Biol. 356, 684–694.
Pastorello, E.A., Pravettoni, V., Farioli, L., Rivolta, F., Conti, A., Ispano, M., Fortunato, D., Bengtsson, A., Bianchi, M., 2002. Hypersensitivity to mugwort (Artemisia vulgaris) in patients with peach allergy is due to a common lipid transfer protein allergen and is often without clinical expression. J. Allergy Clin. Immunol. 110, 310–317.
Pastorello, E.A., Pompei, C., Pravettoni, V., Farioli, L., Calamari, A.M., Scibilia, J., Robino, A.M., Conti, A., Iametti, S., Fortunato, D., Bonomi, S., Ortolani, C., 2003. Lipid-transfer protein is the major maize allergen maintaining IgE-binding activity after cooking at 100 degrees C, as demonstrated in anaphylactic patients and patients with positive double-blind, placebo-controlled food challenge results. J. Allergy Clin. Immunol. 112, 775–783.
Rigby, N.M., Marsh, J., Sancho, A.I., Wellner, K., Akkerdaas, J., van Ree, R., Knulst, A., Fernandez-Rivas, M., Brettlova, V., Schilte, P.P., Summer, C., Pumphrey, R., Shewry, P.R., Mills, E.N., 2008. The purification and characterisation of allergenic hazelnut seed proteins. Mol. Nutr. Food Res. 52 (Suppl 2), S251–261.
Rombouts, I., Lagrain, B., Scherf, K.A., Lambrecht, M.A., Koehler, P., Delcour, J.A., 2015. Formation and reshuffling of disulfide bonds in bovine serum albumin demonstrated using tandem mass spectrometry with collision-induced and electron-transfer dissociation. Sci. Rep. 5, 12210.
Rombouts, I., Lambrecht, M.A., Carpentier, S.C., Delcour, J.A., 2016. Identification of lanthionine and lysinoalanine in heat-treated wheat gliadin and bovine serum albumin using tandem mass spectrometry with higher-energy collisional dissociation. Amino Acids 48, 959–971.
Salcedo, G., Sanchez-Monge, R., Barber, D., Diaz-Perales, A., 2007. Plant non-specific lipid transfer proteins: an interface between plant defence and human allergy. Biochim. Biophys. Acta 1771, 781–791.
Salcedo, G., Sanchez-Monge, R., Diaz-Perales, A., Garcia-Casado, G., Barber, D., 2004. Plant non-specific lipid transfer proteins as food and pollen allergens. Clin. Exp. Allergy 34, 1336–1341.
Sanchez-Lopez, J., Tordesillas, L., Pascal, M., Munoz-Cano, R., Garrido, M., Rueda, M., Vilella, R., Valero, A., Diaz-Perales, A., Picado, C., Bartra, J., 2014. Role of Art v 3 in pollinosis of patients allergic to Pru p 3. J. Allergy Clin. Immunol. 133 1018-1025 e1013.
Sancho, A.I., Rigby, N.M., Zuidmeer, L., Asero, R., Mistrello, G., Amato, S., Gonzalez-Mancebo, E., Fernandez-Rivas, M., van Ree, R., Mills, E.N., 2005. The effect of thermal processing on the IgE reactivity of the non-specific lipid transfer protein from apple, Mal d 3. Allergy 60, 1262–1268.
Scala, E., Till, S.J., Asero, R., Abeni, D., Guerra, E.C., Pirrotta, L., Paganelli, R., Pomponi, D., Giani, M., De Pita, O., Cecchi, L., 2015. Lipid transfer protein sensitization: reactivity profiles and clinical risk assessment in an Italian cohort. Allergy 70, 933–943.
Scheurer, S., Schulke, S., 2018. Interaction of non-specific lipid-transfer proteins with plant-derived lipids and its impact on allergic sensitization. Front. Immunol. 9, 1389.
Scheurer, S., Lauer, I., Foetisch, K., San Miguel Moncin, M., Retzek, M., Hartz, C., Enrique, E., Lidholm, J., Cistero-Bahima, A., Vieths, S., 2004. Strong allergenicity of Pru av 3, the lipid transfer protein from cherry, is related to high stability against thermal processing and digestion. J. Allergy Clin. Immunol. 114, 900–907.
Shenkarev, Z.O., Melnikova, D.N., Finkina, E.I., Sukhanov, S.V., Boldyrev, I.A., Gizatullina, A.K., Mineev, K.S., Arseniev, A.S., Ovchinnikova, T.V., 2017. Ligand binding properties of the lentil lipid transfer protein: molecular insight into the possible mechanism of lipid uptake. Biochemistry 56, 1785–1796.
Stock, L.G., Wildner, S., Regl, C., Gadermaier, G., Huber, C.G., Stutz, H., 2018. Monitoring of Deamidation and lanthionine formation in recombinant mugwort allergen by capillary zone electrophoresis (CZE)-UV and transient capillary Isotachophoresis-CZE-Electrospray Ionization-TOF-MS. Anal. Chem. 90, 11933–11940.
Thing, M., Zhang, J., Laurence, J., Topp, E.M., 2010. Thiol-disulfide interchange in the

tocinoic acid/glutathione system during freezing and drying. J. Pharm. Sci. 99, 4849–4856.
Toda, M., Reese, G., Gadermaier, G., Schulten, V., Lauer, I., Egger, M., Briza, P., Randow, S., Wolfheimer, S., Kigongo, V., Del Mar San Miguel Moncin, M., Fotisch, K., Bohle, B., Vieths, S., Scheurer, S., 2011. Protein unfolding strongly modulates the allergenicity and immunogenicity of Pru p 3, the major peach allergen. J. Allergy Clin. Immunol. 128, 1022–1030 e1021-1027.
Tordesillas, L., Pacios, L.F., Palacin, A., Quirce, S., Armentia, A., Barber, D., Salcedo, G., Diaz-Perales, A., 2009. Molecular basis of allergen cross-reactivity: non-specific lipid transfer proteins from wheat flour and peach fruit as models. Mol. Immunol. 47, 534–540.
van Ree, R., 2002. Clinical importance of non-specific lipid transfer proteins as food allergens. Biochem. Soc. Trans. 30, 910–913.
Vejvar, E., Himly, M., Briza, P., Eichhorn, S., Ebner, C., Hemmer, W., Ferreira, F., Gadermaier, G., 2013. Allergenic relevance of nonspecific lipid transfer proteins 2: identification and characterization of Api g 6 from celery tuber as representative of a novel IgE-binding protein family. Mol. Nutr. Food Res. 57, 2061–2070.
Wijesinha-Bettoni, R., Gao, C., Jenkins, J.A., Mackie, A.R., Wilde, P.J., Mills, E.N., Smith, L.J., 2007. Heat treatment of bovine alpha-lactalbumin results in partially folded, disulfide bond shuffled states with enhanced surface activity. Biochemistry 46, 9774–9784.
Winn, M.D., Ballard, C.C., Cowtan, K.D., Dodson, E.J., Emsley, P., Evans, P.R., Keegan, R.M., Krissinel, E.B., Leslie, A.G., McCoy, A., McNicholas, S.J., Murshudov, G.N., Pannu, N.S., Potterton, E.A., Powell, H.R., Read, R.J., Vagin, A., Wilson, K.S., 2011. Overview of the CCP4 suite and current developments. Acta Crystallogr. D Biol. Crystallogr. 67, 235–242.
Yeats, T.H., Rose, J.K., 2008. The biochemistry and biology of extracellular plant lipid-transfer proteins (LTPs). Protein Sci. 17, 191–198.
Yu, J., Zhou, Y., Tanaka, I., Yao, M., 2010. Roll: a new algorithm for the detection of protein pockets and cavities with a rolling probe sphere. Bioinformatics 26, 46–52.
Zuidmeer, L., van Ree, R., 2007. Lipid transfer protein allergy: primary food allergy or pollen/food syndrome in some cases. Curr. Opin. Allergy Clin. Immunol. 7, 269–273.

Research article

Boiling down the cysteine-stabilized LTP fold - loss of structural and immunological integrity of allergenic Art v 3 and Pru p 3 as a consequence of irreversible lanthionine formation

Sabrina Wildner[a,b], Iris Griessner[a], Teresa Stemeseder[a], Christof Regl[a,b], Wai Tuck Soh[a], Lorenz G. Stock[a,b], Timo Völker[a,b], Claudia Alessandri[c], Adriano Mari[c], Christian G. Huber[a,b], Hanno Stutz[a,b], Hans Brandstetter[a,b], Gabriele Gadermaier[a,b]

[a]Department of Biosciences, University of Salzburg, Salzburg, Austria

[b]Christian Doppler Laboratory for Innovative Tools for the Characterization of Biosimilars, University of Salzburg, Salzburg, Austria

[c]Associated Centers for Molecular Allergology, Rome, Italy

Correspondence

Gabriele Gadermaier

Department of Biosciences

Christian Doppler Laboratory for Biosimilar Characterization

University of Salzburg

Hellbrunner Straße 34, A-5020 Salzburg, Austria

Tel: +43-662-8044-5974, Fax: +43-662-8044-183

Gabriele.Gadermaier@sbg.ac.at

ONLINE MATERIALS AND METHODS

Mass spectrometry

For peptide mass fingerprinting 2 µg of each of the differently treated Art v 3 and Pru p 3 samples (0.30 mg ml^{-1}) were diluted to a concentration of 50 µg mL^{-1} in 150 mmol L^{-1} ammonium acetate (Sigma-Aldrich, Vienna, Austria). Disulfide bonds were reduced by addition of 5 mmol L^{-1} tris(2-carboxyethyl)phosphine hydrochloride (Sigma-Aldrich, Vienna, Austria) and incubation for 15 min at 60°C. Subsequently the cysteine residues were alkylated with 20 mmol L^{-1} iodoacetamide (Sigma-Aldrich, Vienna, Austria) and incubation for 30 min at 22°C. For proteolytic digestion trypsin (porcine pancreas, mass spec grade, Promega, Madison, WI, USA) was added at a ratio of 1:10 (*w/w*) followed by incubation for 3 h at 37°C. The obtained peptides were diluted in H_2O + 0.10% formic acid (*v/v*) to a final concentration of 20 µg mL^{-1}. The injection was carried out in full-loop mode with a sample volume of 5.0 µL (100 ng on column). Separation was carried out employing reversed-phase HPLC on an UltiMate® 3000 Rapid Separation system (Thermo Fisher Scientific, Germering, Germany) equipped with a Hypersil Gold aQ C18 column (100 x 1.0 mm i.d., 1.9 µm, 175 Å) from Thermo Fisher Scientific (Sunnyvale, CA, USA), operated at a temperature of 50°C. Mobile phase A was composed of ultrapure H_2O + 0.10% formic acid (*v/v*), mobile phase B of acetonitrile + 0.10% formic acid (*v/v*). The reversed-phase separation was carried out at a flow rate of 80.0 µL min^{-1} with the following gradient: 2.0% B for 2.0 min, 2.0-10.0% B in 2 min, 10.0-35.0% B in 16 min, column regeneration at 80.0% B for 5 min and re-equilibration at 2.0% B for 20 min. UV-detection was carried out in a 2.4 µL UV-detection cell chamber at 214 nm. The HPLC system was coupled to a Thermo Scientific Q Exactive™ Plus benchtop quadrupole-Orbitrap mass spectrometer *via* an Ion Max™ source with a heated electrospray ionization interface (HESI) both from Thermo Fisher Scientific (Bremen, Germany). Mass spectrometric parameters were set as follows: ESI: source heater temperature of 100°C, spray voltage of 3.5 kV, sheath gas flow of 10 arbitrary units, auxiliary gas flow of 5 arbitrary units, capillary temperature of 300 °C; MS: S-lens RF level of 60.0, AGC target of 1e6, and a maximum injection time of 150 ms. Full scan at a scan range of *m/z* 350–2,000 and a resolution setting of 70,000, followed by five data-dependent HCD scans at 28 NCE at a resolution setting of 17,500.

Mass calibration of the instrument was conducted with Pierce™ LTQ Velos ESI Positive Ion Calibration Solution from Life Technologies (Vienna, Austria). Data evaluation was carried out using Thermo Xcalibur 3.0.63 (Thermo Fisher Scientific) for generating extracted ion current chromatograms, GPMAW 10.10 (Lighthouse data) was employed for generation of *in-silico* proteolytic digests of the respective proteins, and Microsoft Excel version 14.0.7214.5000 was used

for data transfer, relative quantification of peak areas and calculation of mass accuracies. Prior to mass spectrometry of differently treated Art v 3 and Pru p 3 samples at the intact protein level, the protein solutions were desalted with 3 kDa centrifugal filters, re-buffered to ultrapure water and diluted to a concentration of 0.2 mg ml^{-1}. Analysis was carried out on an UltiMate 3000 HPLC system from Thermo Fisher Scientific (Germering, Germany). Proteins were separated at a flow rate of 150 µL min^{-1} on an Atlantis T3 C-18 column (150 × 1.0 mm i.d., 3 µm particle size, 100 Å pore size) from Waters (Milford, MA, USA), operated at a temperature of 50°C. Mobile phase A was H_2O + 0.1% FA, mobile phase B was composed of acetonitrile + 0.1% FA. The reversed-phase separation was carried out with the following gradient: 10.0% B for 2 min, 10.0−30.0% B in 5 min, column regeneration at 80.0% B for 3 min and re-equilibration at 10.0% B for 10 min. 7 µl of sample were injected in in-line split-loop mode. The UV-detection was carried out with a 2.5 µL flow-cell at 214 nm. Mass spectrometry was conducted on a Thermo Scientific™ Q Exactive™ Hybrid-Quadrupol-Orbitrap mass spectrometer equipped with an Ion Max source with a heated electrospray ionization (HESI) probe (Thermo Fisher Scientific, Bremen, Germany). The instrument settings were as follows: source heater temperature of 80°C, spray voltage of 4.0 kV, sheath gas flow of 15 arbitrary units, auxiliary gas flow of 5 arbitrary units, capillary temperature of 300°C, S-lens RF level of 60.0, in-source CID of 20.0 eV, AGC target of 1e6 and a maximum injection time of 200 ms. Proteins were analyzed with a full scan at a scan range of *m/z* 1,000-2,800 and a resolution of 140,000 at *m/z* 200. Deconvolution of the acquired ion spectra was carried out with the Xtract™ algorithm integrated into BioPharma Finder™ version 1.0.76.10 (Thermo Fisher Scientific).

Fourier transform infrared spectroscopy (FTIR)

Secondary structure elements of the non-heated and heated (120 min) Art v 3 and Pru p 3 at both pH conditions were investigated by FTIR. Infrared spectra of Art v 3 and Pru p 3 were recorded at 1.5 mg/ml in 50 mM sodium phosphate pH 3.4 or 7.3 at 25°C using a Tensor II Confocheck FTIR system (Bruker Optics Inc., Billerica, MA, USA) in the range of 3100-1000 cm^{-1}. Protein samples were prepared in an AquaSpec transmission cell connected to a thermostat (Haake F8 thermostat, Thermo Fisher Scientific, Karlsruhe, Germany) with internal temperature control. For each spectrum, a 120 scan interferogram was collected in single beam mode at 4 cm^{-1} resolution. Reference spectra were recorded under identical conditions with only the reference buffer in the cell. The recorded infrared spectra were analyzed by the Protein Dynamics software for Opus 3.0 (Bruker Optics). After baseline correction and vector normalization, the second derivatives of the amide I region were calculated by applying the Savitzky–Golay algorithm with 25 smoothing points.

Determination of the isoelectric point

The isoelectric point (pI) was calculated using the online tool https://web.expasy.org/protparam/.

Size exclusion chromatography

SEC-UV was performed on an UltiMate® 3000 (Thermo Fisher Scientific, MA, USA) equipped with an Acclaim™ SEC-300 pre-column (4.6 x 33 mm; 5 µm particle size; 300 Å pore size) and an Acclaim™ SEC-300 column (4.6 x 300 mm; 5 µm particle size; 300 Å pore size), both from Thermo Fisher Scientific (Waltham, MA, USA). The auto sampler was cooled to 5.0°C. The detection cell volume was 2.5 µl. Separation was performed isocratically with a flow rate of 0.35 ml/min. UV detection was performed at 214 nm with a data rate of 20 Hz. For the calibration curve solutions of albumin, β-lactoglobulin B, cytochrome C, ubiquitin, and L-Phe were prepared in ultrapure water, respectively, at 2.0-3.0 mg/ml. The proteins and the amino acid were combined and diluted with the 100 mM potassium phosphate pH 6.8, 200 mM sodium chloride buffer resulting in a sample mix covering concentrations between 0.033 mg/ml (L-Phe) and 0.13 mg/ml (ubiquitin). Aliquots of Art v 3 and Pru p 3 were diluted with 100 mM potassium phosphate pH 6.8, 200 mM sodium chloride buffer. The nominal mass concentration after the dilution was 0.06 mg/ml for all allergens. 5.0 µl of each sample were injected per run. For data analysis the elution times (linear scale; x-axis) of the calibration mix were plotted against the respective protein/ amino acid molecular weights (logarithmic scale; y-axis). Mass assignment for Art v 3 and Pru p 3 was done by fitting the respective elution times to the calibration curve.

IgG and IgE ELISA measurement

The IgG-binding activity of heated and non-heated Art v 3 and Pru p 3 was investigated in ELISA using a serum pool from mice (n=6) previously immunized with Art v 3 or Pru p 3 [9]. The allergens Art v 3 and Pru p 3 (2 µg/ml) were coated overnight at 4°C to Nunc-Immuno™ Maxisorp ELISA plates (Nalge Nunc, Rochester, NY, USA). Plates were washed twice with 137 mM NaCl, 2.7 mM KCl, 10 mM Tris pH 7.4, 0.5% Tween 20 (TBST) and blocked with TBST, 1% (w/v) BSA for 5 h at room temperature. After the blocking steps, the plates were incubated with a serial dilution (1:200, 1:1000, 1:5000 and 1:25000) of the murine serum pool and incubated overnight at 4°C. Plates were washed five times with TBST and incubated with 1:2000 diluted alkaline phosphatase conjugated rabbit anti-mouse IgG/IgM antibodies (Jackson ImmunoResearch, Cambridgeshire, UK) for 1 h at 37°C and 1 h at 4°C. After four TBST buffer washes, plates were developed with the substrate 4-Nitrophenyl-phosphate (Sigma-Aldrich, St Louis, MO, USA) in AP detection buffer (1 M

diethanolamin, 1 mM $MgCl*6H_2O$, pH 9.8). The optical density was measured at 405/492 nm using a microplate reader (SLT Spectra 1.1, TECAN, Grödig, Austria).

The IgE-binding activity of heated and non-heated Art v 3 and Pru p 3 was investigated in ELISA using sera from twenty-six mugwort pollen and peach allergic patients. Purified Art v 3 and Pru p 3 (4 µg/ml) was coated overnight at 4°C to Nunc-Immuno™ Maxisorp ELISA plates (Nalge Nunc, Rochester, NY, USA). After the washing and blocking steps, patients´ sera were diluted 1:5 in TBST, 0.5% (w/v) BSA and incubated overnight at 4°C. Plates were washed five times with TBST and incubated with 1:2000 diluted alkaline phosphatase conjugated monoclonal mouse anti-human IgE antibodies (BD Bioscience, San Diego, CA, USA) for 1 h at 37°C and 1 h at 4°C. The rest of the ELISA was carried out analogous to the IgG ELISA.

ONLINE TABLES AND FIGURES

Online Table 1: Crystallographic data and refinement statistics.

PDB Code	**6FRR**
Structure	**Art v 3**
Data collection	
Wavelength (Å)	0.8856
Unit cell parameters	
a, *b*, *c* (Å)	60.40, 60.40, 91.46
α, *β*, *γ* (degrees)	*α* = *β* = *90 γ* = 120
Space group	$P3_2$ 2 1
Solvent content (%)	47.42
Protein chains in AU	2
Resolution range (Å)	52.31–1. 95
Highest resolution shell (Å)	2.05–1.95
Unique reflections	14,608 (2087)
Multiplicity	6.4 (10)
Completeness (%)	99.7 (99.9)
$*R_{merge}$	0.083 (0.31)
Average $I/\sigma(I)$	17.2 (6.7)
Refinement	
R_{work} (%)	19.28
R_{free} (%)	24.94
Mean B value (Å^2)	27
B from Wilson plot (Å^2)	25.7
RMSD bond length (Å)	0.007
RMSD bond angles (degrees)	0.828
No. of amino acid residues	92
No. of water molecules	194
Ramachandran plot	
Most favored regions (%)	98
Additional allowed regions (%)	2

Values of highest resolution shell are given in parenthesis. $*R_{merge} = \Sigma_h\Sigma_j |I_{hj} - \langle \tilde{o} I_h \rangle| / \Sigma_h\Sigma_j |\langle I_h \rangle|$

Online Table 2: Demographic information and allergy related patients' data.

No.	Age	Gender	Symptomes	Art v 3 [ISU-E]	Pru p 3 [ISU-E]
1	43	M	OAS	1.16	3.21
2	17	F	OAS	0.95	5.92
3	14	F	OAS	11.11	11.90
4	36	F	AP	3.28	3.39
5	21	M	U	6.93	8.50
6	26	M	A, OAS, U	3.11	6.60
7	31	M	OAS, U	3.25	3.61
8	24	M	A, OAS, U	3.23	6.53
9	15	M	A, OAS, U	5.17	18.71
10	33	F	OAS	5.60	21.18
11	19	M	OAS	6.05	0.56
12	18	F	A, OAS, U	5.27	5.20
13	30	F	ANX, OAS, U	6.21	9.22
14	14	M	ANX, OAS, U	9.23	9.85
15	26	M	A, U	7.62	9.18
16	27	M	ANX, OAS, U	6.23	9.26
17	28	F	A, U	23.50	1.04
18	24	M	OAS	15.93	3.09
19	48	F	ANX, OAS, U	6.31	6.92
20	44	F	OAS	14.58	2.74
21	49	F	OAS	0.40	3.28
22	32	F	OAS, U, ANG	4.65	8.88
23	23	F	OAS, U	1.15	1.71
24	36	M	OAS, U	0.12	1.42
25	38	F	OAS	0.8	0.13
26	23	F	ANX, OAS, U, ANG	2.22	3.63

OAS, oral allergy syndrome; U, urticaria; AP, abdominal pain; A, asthma; ANX, anaphylaxis; ANG, angioedema; ISU-E, ISAC standardized units of IgE

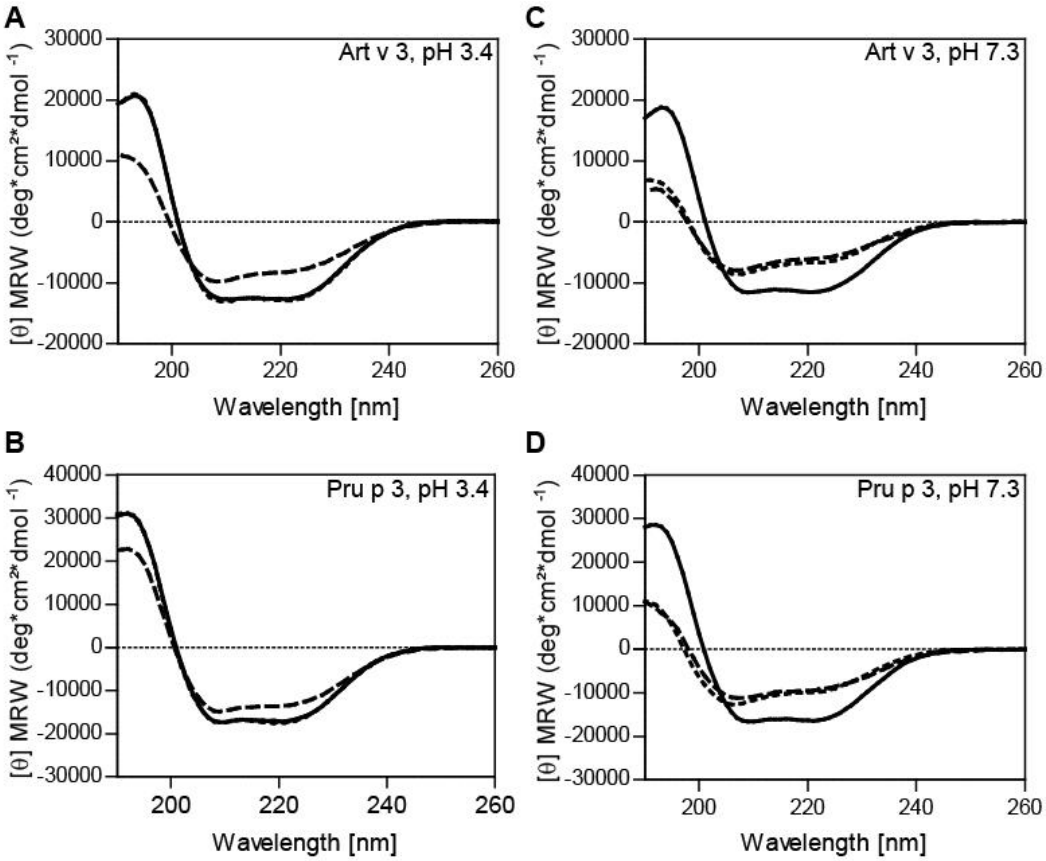

Online Fig. E1: Secondary structure analysis of native Art v 3 and Pru p 3 using CD spectroscopy. CD spectra of native Art v 3 at pH 3.4 (A), Art v 3 at pH 7.3 (B), Pru p 3 at pH 3.4 (C) and Pru p 3 at pH 7.3 (D) were recorded at 20°C, 95°C and 20°C after renaturation. Solid lines represent spectra recorded at 20°C, long and short dashed lines were spectra recorded at 95°C and 20°C after denaturation, respectively.

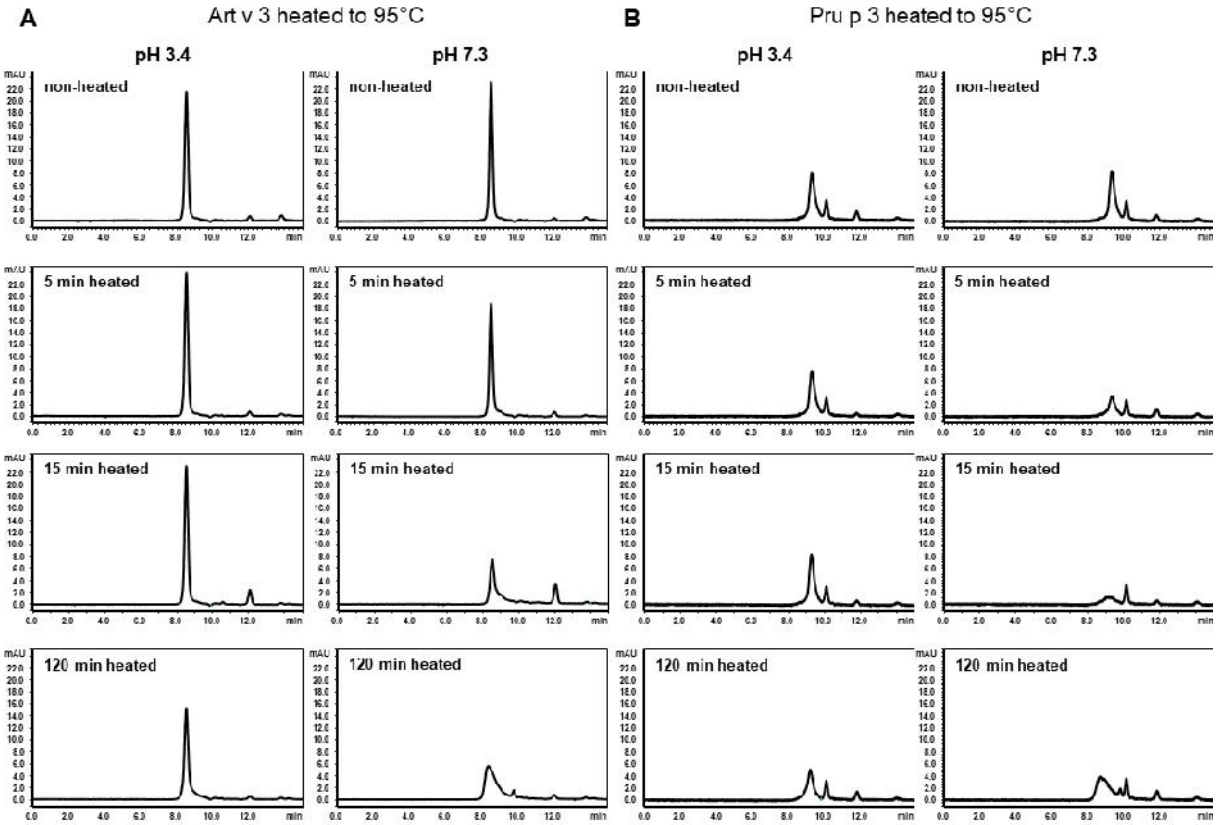

Online Fig. E2: Response of two non-specific lipid transfer proteins to heat treatment under different pH conditions. SEC data of Art v 3 (A) and Pru p 3 (B) after heating to 95°C in 10.0 mM phosphate buffer adjusted to pH 3.4 or pH 7.3. A non-heated control and samples heated for 5 min, 15 min, and 120 min were analyzed, respectively. SEC-UV: Column: Acclaim™ SEC-300 (4.6 x 300 mm), particle size 5 µm, pore size 300 Å. Pre-column: Acclaim™ SEC-300 (4.6 x 33 mm) particle size 5 µm, pore size 300 Å. Eluent: 100.0 mM potassium phosphate buffer + 200 mM NaCl. pH 6.80±0.05. Flow rate: 0.350 ml/min isocratically for 15.0 min. Injection: 5.0 µL. Detection: 214.0 nm with a data rate of 20 Hz. Detection cell volume: 2.5 µL.

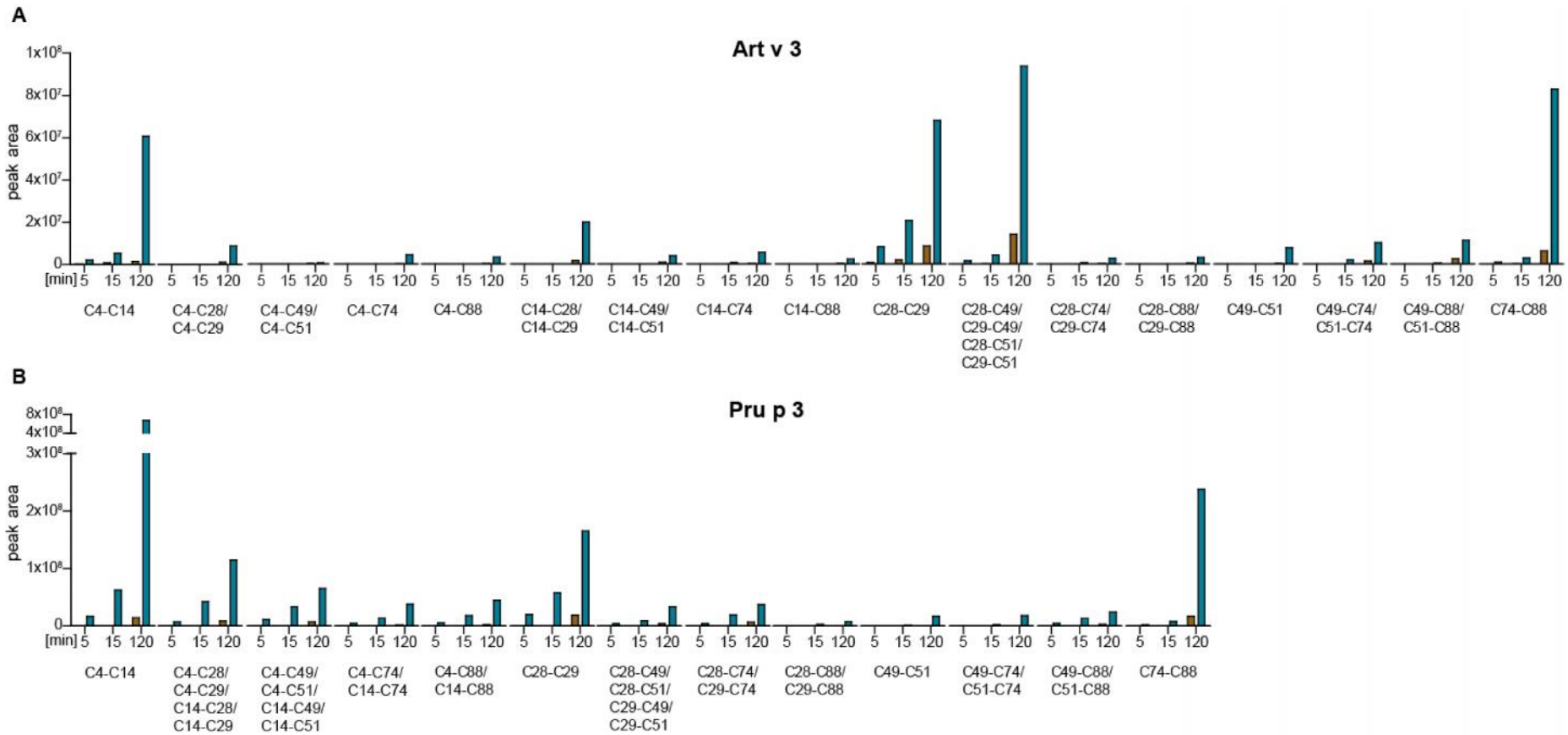

Online Fig. E3: Semi-quantitative mass-spectrometry based analysis of lanthionine containing peptides upon thermal treatment at acidic (pH 3.4, beige bars) and neutral (pH 7.3, cyan bars) conditions. No lanthionine formation was detectable at time point zero. Lanthionine formation was more prominent in distinct peptides upon treatment at neutral conditions, while induction was generally very low at pH 3.4.